



**CHARLES UNIVERSITY**  
Faculty of Pharmacy  
in Hradec Králové

*Department of Pharmaceutical Technology*

**CHARACTERIZATION OF PLGA-BASED  
FILM FORMING SYSTEMS**

*Rigorous thesis*

Hereby I declare that this rigorous thesis is my original author work and was compiled under the supervision of PharmDr. Eva Šnejdrová, Ph.D. using only the listed literature and sources. Further I declare that this rigorous thesis has not been used to obtain any other or the same academic title.

I would like to express my sincere thanks to PharmDr. Eva Šnejdrová, Ph.D. for her professional leadership, friendly attitude and help with elaboration of this thesis.

Special thank goes to my employer, PharmDr. Vladimír Müller, who kindly supports continuous education of the team.

Hradec Králové 2021

Mgr. Andrea Věříš

# TABLE OF CONTENTS

ABSTRACT .....	6
ABSTRAKT .....	7
AIM OF THE RIGOROUS THESIS .....	8
ABBREVIATIONS .....	9
INTRODUCTION.....	10
1 THEORETICAL PART .....	11
1.1. Introduction to film forming systems .....	11
1.2. Mechanism of film formation.....	11
1.3. Components of FFSs .....	13
1.3.1. Drug.....	13
1.3.2. Solvent.....	13
1.3.3. Polymer .....	14
1.3.4. Plasticizer .....	16
1.4. Components of formulated PLGA-based FFSs .....	17
1.4.1. Acidum salicylicum.....	17
1.4.2. PLGA derivatives .....	17
1.4.3. Plasticizers.....	18
1.5. Testing of FFSs.....	19
1.5.1. Drying time .....	19
1.5.2. Film thickness .....	19
1.5.3. Tensile strength .....	19
1.5.4. Film tackiness.....	20
1.5.5. Water resistance test.....	20
1.5.6. Gas permeability .....	20
1.5.7. Fourier transform infrared analysis .....	20
1.5.8. Thermal analyses.....	20

1.5.9. Microstructural analysis .....	21
1.5.10. Drug release.....	21
1.5.11. Rheological characterization .....	21
1.6. Adhesive properties .....	22
1.6.1. Peel off test.....	22
1.6.2. Tensile tests .....	22
1.6.3. In vivo adhesion testing.....	22
1.7. Mathematical models for evaluation of flow behavior.....	23
1.7.1. Newton model .....	23
1.7.2. Power law model.....	24
1.7.3. Sisko model .....	24
1.7.4. Cross model.....	25
2 EXPERIMENTAL PART .....	26
2.1. Materials .....	26
2.1.1. Substances .....	26
2.1.2. Devices .....	26
2.2. DSC .....	27
2.3. Rheological testing .....	27
2.3.1. Rotation testing .....	28
2.3.2. Oscillation testing.....	28
2.4. Adhesion.....	29
2.5. SEM.....	29
2.6. FFS formulation.....	29
2.7. Drug release .....	30
3 RESULTS.....	31
3.1. DSC .....	31
3.2. Rheological characterization .....	35

3.2.1. Viscosity curves .....	35
3.2.2. Values of consistency index, power law index a shear viscosity.....	39
3.2.3. Oscillation .....	41
3.3. Adhesive properties .....	44
3.4. SEM.....	48
3.5. Drug release.....	50
4 DISCUSSION .....	53
4.1. DSC .....	53
4.2. Rheological testing .....	53
4.3. Adhesion.....	56
4.4. SEM.....	57
4.5. Drug release.....	57
5 CONCLUSIONS.....	60
6 ACNOWLEGEMENTS.....	61
7 REFERENCES.....	62

## ABSTRACT

Title of thesis: Characterization of PLGA-based film forming systems  
Author: Mgr. Andrea Věříš  
Department: Department of Pharmaceutical Technology  
Supervisor: PharmDr. Eva Šnejdrová, Ph.D.

The aim of this thesis is to review available sources on film forming systems (FFSs), to test characteristics of poly(lactic-*co*-glycolic acid) of low molar mass linear or branched configuration in combination with multifunctional plasticizers and to formulate salicylate loaded film forming system. The theoretical section is focused on general characteristics and excipients used for FFs formulation and testing methods. Besides that, mathematical models commonly used for evaluation of flow behaviour are included.

In the experimental section, effects of plasticizers ethyl pyruvate, methyl salicylate and triacetin on the rheological and adhesive properties of the polyesters were tested to select the optimal combination. All tested plasticizers decrease the viscosity of the polymers with ethyl pyruvate being the most effective. The flow curves of plasticized PLGA were analysed to Power law and Newton models revealing the Newton character of the systems. The evaluation of viscoelastic behavior showed liquid-like characteristic of these systems. The adhesive properties were determined by the pull away test providing the detachment force and time necessary for force to decrease by 90%. The highest adhesiveness was found in case of the most viscous systems. FFSs loaded with salicylic acid were prepared and their structure was studied with SEM showing good homogeneity. The images confirmed molecularly dispersed drug in PLGA determined by DSC. Finally, the dissolution of salicylates was tested. Prolonged release of salicylates within 11 days was found with a linear pattern within first 5 days.

**Keywords:** film forming system, branched polyesters, plasticizer, rheological properties, adhesive properties

## ABSTRAKT

Název práce: Hodnocení vlastností soustav pro tvorbu tenkých filmů založených na PLGA

Autor: Mgr. Andrea Věříš

Katedra: Katedra farmaceutické technologie

Konzultant: PharmDr. Eva Šnejdrová, Ph.D.

Cílem práce je prezentovat dostupné informace týkající se systémů pro formulaci *in situ* filmů (FFSs), testovat vlastnosti kyseliny poly(mléčné-*ko*-glykolové) s nízkou molární hmotností lineární nebo rozvětvené konfigurace v kombinaci s multifunkčními plastifikátory a formulovat FFSs s kyselinou salicylovou. Teoretická část je zaměřena na obecné charakteristiky a pomocné látky používané pro formulaci FFSs a metody jejich testování. Dále jsou zahrnuty matematické modely používané pro matematický popis tokových křivek.

V experimentální části byl studován vliv plastifikátorů ethylpyruvátu, methylsalicylátu a triacetinu na reologické a adhezivní vlastnosti PLGA. Nejúčinnějším plastifikátorem byl ethylpyruvát. Analýza tokových křivek potvrdila Newtonovský charakter plastifikovaných polyesterů s viskozitou nezávislou na rychlostním spádu. Oscilační testy prokázaly, že plastifikované PLGA deriváty jsou viskoelastické kapaliny. Adhezivní vlastnosti byly stanoveny tahovým testem a vyhodnoceny pomocí maximální síly a času potřebného pro snížení síly o 90 %. Nejvyšší adheze byla zjištěna u systémů s nejvyšší viskozitou. Byly připraveny FFSs s kyselinou salicylovou a jejich struktura studována pomocí SEM. Snímky ukázaly dobrou homogenitu filmů a potvrdily výsledky DSC, které prokázaly, že léčivo je v polymeru molekulárně dispergované. V disolučním testu bylo zjištěno prodloužené uvolňování salicylátů po dobu 11 dnů s lineárním průběhem během prvních 5 dnů.

**Klíčová slova:** filmtvorné systémy, větvené polyestery, plastifikátor, reologické vlastnosti, adhezivní vlastnosti.

## **AIM OF THE RIGOROUS THESIS**

The overall aim of this thesis is to review available sources on film forming systems (FFSs), to test characteristics of poly(lactic-*co*-glycolic acid) of low molar mass linear or branched configuration in combination with multifunctional plasticizers and to formulate salicylate loaded film forming system.

The assignment can be concretized into these steps:

1. Testing of polyesters with different molar weight for formulation of FFS, specifically: linear PLGA polyester and PLGA branched on triptaerythritol (3T), polyacrylic acid (2A) or dipentaerythritol (8D).
2. Plasticization of PLGA derivatives with ethyl pyruvate, methyl salicylate or triacetin.
3. Testing of the thermal, rheological and adhesive properties of non-plasticized and plasticized polyesters.
4. Selection of the most suitable polymer and plasticizer for formulation of the FFSs with drug.
5. Testing of dissolution of salicylates from FFS.



## ABBREVIATIONS

2A	poly(lactic- <i>co</i> -glycolic acid) branched with dipentaerythritol
3T	poly(lactic- <i>co</i> -glycolic acid) branched with tripentaerythritol
8D	poly(lactic- <i>co</i> -glycolic acid) branched with polyacrylic acid
AFM	atomic force microscopy
DSC	differential scanning calorimetry
EP	ethyl pyruvate
FFS	film forming system
FFSs	film forming systems
FTIR	Fourier transform infrared analysis
MS	methyl salicylate
PBS	phosphate-buffered saline
PLGA	poly(lactic- <i>co</i> -glycolic acid)
SEM	scanning electron microscopy
TA	triacetin
TGA	thermogravimetric analysis

## INTRODUCTION

As the largest organ of the human body skin represents an ideal and easily accessible target for the application of topical preparations whether for local or systemic treatment. The use of the conventional topical dosage forms such as semisolids (creams, ointments, gels etc.) and patches is limited by some of their undesirable characteristics. Patches often cause skin irritation due to their occlusive properties resulting in sweat-duct obstruction, they are difficult to apply on uneven surfaces, their removal might cause pain and aesthetic appeal is rather negative. Semisolid formulations overcome some of these difficulties but get wiped-off easily and the applied amount is strongly influenced by the patients, thus the delivery of therapeutically effective doses is not guaranteed. Film forming system (FFS) as a novel dosage form overcomes some of the previously mentioned drawbacks of the conventional ones and its potential is to be developed yet. The relatively short period of its use is also reflected in the lack of standardized testing methods for the finished dosage form. This work studies the rheological, thermal and adhesive properties of poly(lactic-*co*-glycolic acid) polyesters of branched architecture in relation to their potential for use in FFSs together with basic characteristics of formulated model FFS.

# 1 THEORETICAL PART

## 1.1. Introduction to film forming systems

Film forming system (FFS) is a novel approach to the transdermal and dermal drug delivery being an alternative to the current topical preparations. It is described as a non-solid dosage form that produces a film *in situ* i.e. after application on the skin or other body surface. These systems are composed of active substance and film-forming ingredients diffused in a vehicle which evaporates or absorbs rapidly in the stratum corneum (SC) leaving behind an adhesive film of excipients along with the drug<sup>1</sup>. The first film-forming solution, isopropanol solution containing testosterone and combination of two polymers - polyvinylpyrrolidone and polyvinyl alcohol, was described in 1996 by Amit Misra et al. and since then the category has undergone extensive development by several research teams at both academic institutions as well as pharmaceutical companies<sup>2-4</sup>.

Besides the fact that film forming systems (FFSs) overcome some of the drawbacks of conventional topical products such as occlusion of sweat-ducts and painful removal (patches) or easy wipe-off leading to subtherapeutical drug levels (creams, ointments, gels), they can also act as a drug reservoir reducing the frequency of necessary application and thus improving the patient compliance<sup>1,5,6</sup>. Additionally, their cosmetic aspects may be more appealing than those of semisolids as they are fast drying, less greasy and more discrete thanks to the transparency<sup>7</sup>.

Currently some FFS preparations for local treatment of dermatologic diseases (terbinafine hydrochloride)<sup>8</sup> or pain management (combination of lidocaine and tetracaine)<sup>9</sup> as well as for systemic therapeutic effects (estradiol)<sup>10</sup> are marketed with others being in the phase of clinical testing<sup>11</sup>.

## 1.2. Mechanism of film formation

The formation of the film begins just after the application when the first molecules of solvent start to evaporate. Depending on the solubility of film forming polymer in the used solvent, the FFSs can be either solutions or dispersions. This subsequently influences the process of film formation<sup>1</sup>. While the polymer chains in the solution are intimately mixed and film formation occurs as the solvent evaporates, the polymer particles in a dispersion must first coalesce to enable the interpenetration of the individual polymer chains (**Figure 1**). The coalescence is caused by the with solvent evaporation increasing capillary forces<sup>12,13</sup>.

The initial state of polymer also influences the properties of the final film. Polymer solutions usually result in a transparent, smooth film whereas the films formed from the dispersion, especially emulsion, might be opaque with rough surface. In both cases the use of plasticizer is common to improve the properties of the final film<sup>4,12</sup>.

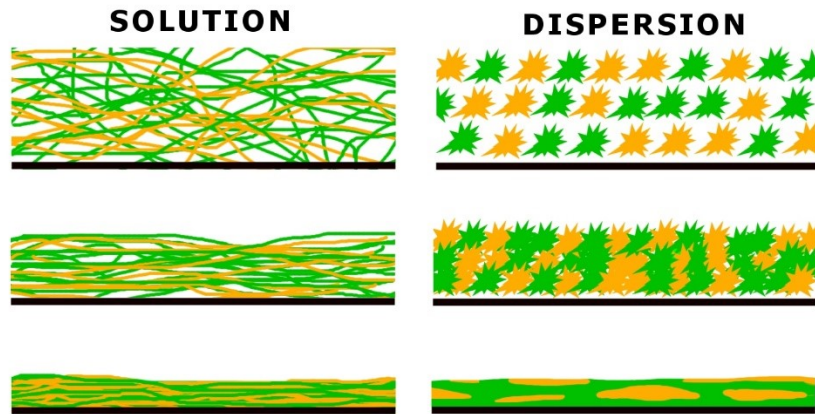


**Figure 1** Schematic illustration of the mechanism of polymeric film formation from a FFS solution and dispersion. Image modified based on <sup>12</sup>.

Besides the film formation, the evaporation of volatile solvents leads to the significant loss of volume and consequently to the rapid increase in concentration of active substance in the formulation<sup>12</sup>. This positive change of concentration might generate supersaturation which improves the drug permeation across the skin without the necessity to use enhancers. The effect of supersaturation can be explained by an adapted form of Fick's law of diffusion given by the equation below<sup>6</sup>:

$$J = \frac{DKC_v}{h} \quad (1)$$

where

- J rate of drug permeation (the flux) [ $\text{mol}\cdot\text{cm}^{-2}\cdot\text{s}^{-1}$ ]
- D diffusion coefficient of the drug [ $\text{cm}^2\cdot\text{s}^{-1}$ ]
- K partition coefficient of the drug, dimensionless
- $C_v$  concentration of the drug in the vehicle [ $\text{mol}\cdot\text{cm}^{-3}$ ]
- H diffusional pathlength [cm]

### 1.3. Components of FFSs

All substances used for formulation of FFSs influence the mechanical and cosmetic properties of the final film as well as the drug delivery. Some of their effects are well described and might be used for selection prior to development whereas others cannot be predicted and should be determined on case-by-case basis<sup>12</sup>.

#### 1.3.1. Drug

To be able to penetrate the skin - efficient barrier protecting human body from external agents - the drug molecule needs to fulfill certain requirements. Its molecule should be small (< 500)<sup>14</sup>, neither very hydrophilic, nor too lipophilic (Log P = 1 – 3)<sup>15</sup> and preferably uncharged (pH 5 – 9 in aqueous solution). Other advantageous parameters are small number of hydrogen bonding groups (< 2) and a low melting point<sup>16</sup>.

Besides the above-mentioned factors independent of the dosage form also the specifics of FFS have to be considered. The size of drug reservoir is limited by the thinness of the film ( $\mu\text{m}$ ) and application area (practically tens of  $\text{cm}^2$ ). Also, drug loading capacity of the FFS and absorption rate set limits for the amount of drug delivered. Based on this the FFSs for transdermal delivery will be mainly attractive for drugs, that show<sup>17</sup>:

- high potency
- high skin permeability
- high solubility in the solvent

The active substances designated for local treatment are obviously exempt of the requirements for transdermal delivery which is in this case undesirable. Therefore, the key factor is good solubility in solvent and polymer, which should prevent their crystallization.

#### 1.3.2. Solvent

As the carrier medium, solvents often form the major part of FFS, especially in film forming solutions. The right solvent should provide sufficient solubility for both polymer and drug ensuring satisfactory drug loading capacity<sup>17</sup>. One of the most important characteristics of FFS highly influenced by solvent is drying time which should be up to 5 minute to minimize patients discomfort<sup>18</sup>. Therefore, highly volatile organic solvents are preferred<sup>12</sup>. Among them, ethanol is solvent of choice because of the fact that main regulatory agencies allow it for topical use in concentrations > 95%<sup>19</sup>. Most commonly used solvents including their mixtures reported in literature are summarized in the **Table 1**.

**Table 1** Examples of solvents frequently used in FFSs.

Category	Examples
Alcohols	Ethanol, Isopropyl alcohol
Glycols	Propylenglycol
Others	Water, butyl acetate, ethyl acetate, dibutyl phthalate

### 1.3.3. Polymer

Polymers are the core components of FFSs enabling the actual formation of the film. They should be selected considering the compatibility with the drug and its stability, delivery and final therapeutic effect. Also, polymers affect visual attributes of the final film and together with plasticizers determine its mechanical properties and adhesion.

For use in FFSs, polymers should ideally fulfil the following<sup>3</sup>:

- biocompatibility
- compatibility with the active substance
- ability to form clear film at the skin temperature (28 – 32 °C)
- sufficient flexibility and adhesion to the skin surface
- sufficient acceptance of active substance to enable creation of drug reservoir
- solubility in highly volatile, non-irritating solvents

In past three decades various commercially available polymers (**Table 2**) were tested for *in situ* FFSs with many of them showing satisfactory results. The most commonly used are cellulose and methacrylic derivates which cover a wide range of polarity<sup>20</sup>.

**Table 2** Overview of polymers tested for FFS as reported in the literature.

Group	Chemical name Commercial name	Solubility water	Solubility ethanol	Polarity
Cellulose derivatives	Hydroxypropyl methylcellulose <i>Metolose 90SH-4000</i> <sup>20</sup>	Yes (cold)	Yes	Hydrophilic
	Hydroxypropyl cellulose <i>Klucel™ LF</i> <sup>3,7</sup> <i>Klucel™ HF</i> <sup>20</sup>	Yes (cold)	Yes	Hydrophilic
	Ethyl cellulose <i>Ethocel standard 20 Premium</i> <sup>21</sup> <i>Ethocel standard 10FP premium</i> <sup>22</sup> <i>Aqualon EC N10/N22/N50</i> <sup>7</sup>	No	Yes	Hydrophobic
Poly(meth)acrylates	Polymethacrylates <i>Eudragit® E100</i> <sup>3,20</sup> <i>Eudragit® L100</i> <sup>20</sup> <i>Eudragit® L100-55</i> <sup>20</sup> <i>Eudragit® NE 30D</i> <sup>23</sup> <i>Eudragit® NE 40D</i> <sup>3,7</sup> <i>Eudragit® RL100</i> <sup>21</sup> <i>Eudragit® RL PO</i> <sup>3</sup> <i>Eudragit® RS100</i> <sup>21,22</sup> <i>Eudragit® RS 30D</i> <sup>23</sup> <i>Eudragit® RS PO</i> <sup>7</sup> <i>Eudragit® S 100</i> <sup>3</sup>	No	Yes	Lipophilic
	Polyacrylates <i>Dermacryl® 79</i> <sup>3,7</sup> <i>Avalure® AC 118</i> <sup>3</sup>	No	Yes	Lipophilic
Lactic acid polymers	Poly(lactic-co-glycolic) acid <i>EXPANSORB® DLG 50-2A/50-5A/50-8A/75-5A</i> <sup>24</sup>	No	No	Lipophilic
Vinyl polymers	Polyvinyl pyrrolidone <i>Kollidon® 12PF/17PF/25/30</i> <sup>3,7</sup> <i>PVA and PVP K30</i> <sup>*18</sup> <i>Kollidon® VA 64</i> <sup>3</sup>	Yes	Yes	Hydrophilic
	Polyvinyl alcohol <i>PVA and PVP K30</i> <sup>*18</sup> <i>PVA 7200</i> <sup>3</sup>	Yes	Yes	Hydrophilic
Chitosan	Chitosan <i>Chitofarm® S/M</i> <sup>7</sup> <i>Hydagen® HCMF</i> <sup>3</sup>	No	No	Hydrophilic
Others	Silicon gum <i>SGM 36</i> <sup>3</sup>	No	No	Lipophilic
	Polyisobutylene <i>Oppanol® B100 / 10SFN</i> <sup>3</sup>	No	No	Lipophilic
	Tamarind seed gum (carboxymethylated) <sup>25</sup>	Yes	No	Hydrophilic

\*mixture of PVP+PVA

The list of tested polymers is expected to expand due to still ongoing research and necessity to provide sufficient selection for potential development of this type of finished dosage form.

### 1.3.4. Plasticizer

To improve the mechanical properties of the polymer and/or the final film, addition of a plasticizer is often necessary. Typically, low-molecular compounds are used (Table 3), increasing the flexibility of the polymer. This is achieved by incorporation of plasticizer molecules between the polymer chains which leads to increase in the free volume and free chain movement and consequently reduction of the glass transition temperature ( $T_g$ ) and the minimum temperature of film formation<sup>12,26</sup>. Considering the skin application, the final  $T_g$  should be ideally below 32 °C to ensure the flexibility (and thus adaptability to skin movements) of the formed film<sup>12</sup>. Besides the modification of mechanical properties plasticizers can also influence the drug release from the film<sup>7</sup>.

**Table 3** Examples of plasticizers frequently used for pharmaceutical applications.

Triethyl citrate <sup>3,7,20,27</sup>	Glycerol <sup>22,24,25</sup>
Tributyl citrate <sup>7,28</sup>	Polyethylene glycol 400 <sup>22,24,25</sup>
Dibutyl phthalate <sup>3,28</sup>	Propylene glycol <sup>24</sup>
Diethyl phthalate <sup>28</sup>	Medium chained triglycerides <sup>20</sup>
Dibutyl sebacate <sup>7,27</sup>	Urea <sup>29</sup>
Triacetin <sup>3,21,28</sup>	

Furthermore, the plasticizer itself might possess some pharmacological activity which might support the effect of the treatment. In the scope of this work three plasticizers with additional, potentially beneficial, activities were tested:

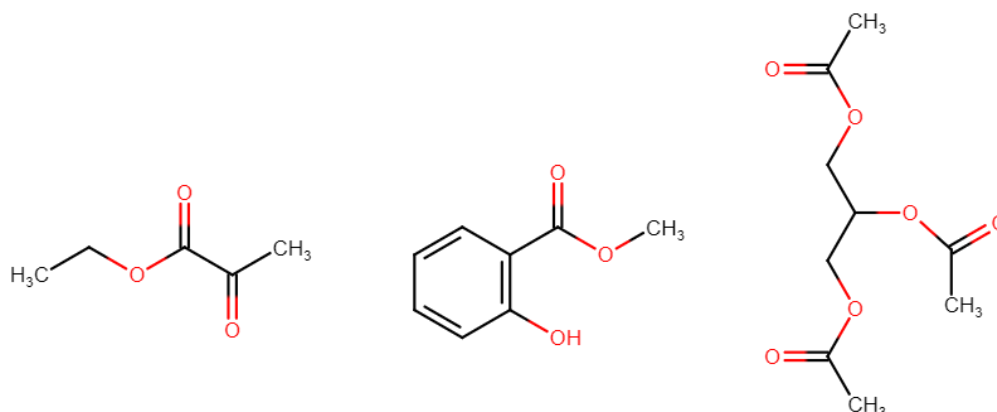


**Figure 2** Formula of ethyl pyruvate, methyl salicylate and triacetin (from left to right)



## 1.4. Components of formulated PLGA-based FFSs

### 1.4.1. *Acidum salicylicum*

Salicylic acid is an active pharmaceutical ingredient with small molecule originally obtained from the bark of white willow (*Salix alba*) which lent it the name. It is a beta hydroxy acid, derivate of benzoic acid, with molecular weight of 138.12. It has analgesic, anti-inflammatory and keratolytic activity<sup>30</sup>. The mechanism of its anti-inflammatory activity, inhibition of enzyme cyclooxygenase and with that prostaglandin synthesis, was described in 1971 by Vane et al.<sup>31</sup>. Keratolytic activity is explained by the reduction of intercellular cohesion between corneocytes by dissolving the intercellular cement in the stratum corneum<sup>32</sup>. However, it was proved that salicylic acid also possesses keratoplastic activity<sup>33</sup> resulting in thickening of keratin layer with the determining factor between keratolytic and keratoplastic effect being the concentration. Below 3% in concentration the effect is keratoplastic, above this value keratolytic<sup>34</sup>. Further important activity shown by salicylic acid is its antioxidative property caused by the ability to trap hydroxyl radicals<sup>35</sup>. Currently, salicylic acid is the most commonly used keratolytic substance and also promotes the skin availability of other topical therapies<sup>32</sup>. When combined with methyl salicylate a considerable amount of salicylic acid may be absorbed through the skin even after topical application<sup>36</sup>.

### 1.4.2. *PLGA derivatives*

Poly(lactic-*co*-glycolic acid) (PLGA) belongs to the family of biodegradable polymers which are successfully used for production of bioresorbable surgical sutures, supportive material in tissue engineering and lately also of drug delivery systems. Besides high biocompatibility, tunable physicochemical properties and proven safety the key benefit of PLGA might be its approval by FDA and EMA<sup>37</sup>.

Tested polymers were prepared by the direct melt polycondensation of equimolar quantities of D,L-lactic and glycolic acids without or with branching agent resulting in linear resp. branched polymers. The branched polyesters are designated by number – percentage of branching agent, and capital letter – branching agent type (D – dipentaerythritol, T – tripentaerythritol, A – polyacrylic acid)<sup>38</sup>. The important characteristics of all polymers are summarized in the **Table 4**.

**Table 4** The physicochemical characteristics of the polymers used for formulation of FFS

Polyester	$M_n$ (g/mol)	$M_w$ (g/mol)	$[\eta]_w$ (mL/g)	$g'$
PLGA 50:50	1,700	2,400	5.9	1.0
8D	1,600	2,500	2.9	0.45
2A	8,600	14,400	8.9	0.54
3T	5,300	17,400	7.7	0.43

D – dipentaerythritol, T – tripentaerythritol, A – polyacrylic acid,  $M_n$  -number-average molar mass,  $M_w$  – weight-average molar mass,  $g'$  - branching ratio

### 1.4.3. Plasticizers

#### *Triacetin (TA) (CAS: 102-76-1)*

Pharmacopeial compound with IUPAC name 2,3-diacetyloxypropyl acetate (**Figure 2**), generally known as triacetin, belongs to the family of triglycerides<sup>39</sup>. Although it occurs naturally in cod-liver oil, butter or other fats, it's synthesized for industrial purposes<sup>40</sup>. Under normal conditions (25 °C, 100 kPa) it is a viscous, colorless and odorless liquid with high boiling point<sup>39</sup>. It is commonly used as a food additive<sup>41</sup>, cosmetic ingredient<sup>40</sup> and excipient in the pharmaceutical industry<sup>39</sup>, especially as a plasticizer, humectant or solvent. Besides that, it has proven antifungal activity<sup>42</sup> which might be beneficial if used as plasticizer in topical antifungal FFSs.

#### *Ethyl pyruvate (EP) (CAS: 617-35-6)*

Small molecule with IUPAC name ethyl 2-oxopropanoate (**Figure 2**) is an ester of endogenous metabolite, pyruvic acid. Under normal conditions it is a colorless liquid with sweet floral odor and high boiling temperature<sup>43</sup>. Being an important intermediate, it is widely used in pharmaceutical and chemical industry for synthesis of drugs, pesticides, resins and plastics. Thanks to its pleasant aroma and skin conditioning properties it is used itself in fragrances and cosmetic products<sup>44</sup>. Moreover, in 2002 Yang et al. described its anti-inflammatory activity in mice model<sup>45</sup>. Since then its anti-inflammatory activity was proven in other *in vivo* and *in vitro* models<sup>46-49</sup>.

#### *Methyl salicylate (MS) (CAS: 119-36-8)*

A pharmacopeial organic ester of salicylic acid with IUPAC name methyl 2-hydroxybenzoate is a naturally occurring substance, first extracted in 1843 from *Gaultheria procumbens*. Nowadays it's production for industrial use is mostly synthetic. Under normal conditions it is a colorless, yellowish or reddish oily liquid having typical odor of wintergreen<sup>50</sup>. It has a boiling point of 220 – 224 °C. Because of its odor and taste it's widely used as a flavoring agent in food

industry as well as fragrance and denaturant in cosmetics<sup>51</sup>. Besides perfuming its utilization in cosmetics is supported by its warming effect and fact, that methyl salicylate, as a precursor of salicylic acid, possesses certain anti-inflammatory and keratolytic properties<sup>51</sup>. Thanks to this activity, it is also used in medicinal topical products designated for pain relief and treatment of muscle or joint soreness<sup>52</sup>.

## **1.5. Testing of FFSs**

Being a novel dosage form there is no specific testing for FFSs set in pharmacopoeias yet. Currently it would fall under the general category of liquid preparations for cutaneous application as defined in European Pharmacopoeia<sup>53</sup>. Nevertheless, this does not provide any guidance for quality control of final films. In available literature several methods were used and described and will be summarized below.

### **1.5.1. Drying time**

Drying time is a crucial parameter of FFSs with great influence on patient's compliance. As stated by Khasraghi et al. the drying time should not be longer than 5 minutes to minimize patient's discomfort<sup>18</sup>. The test itself is not complicated - prescribed quantity of FFS preparation is applied on a non-stick surface, usually glass or teflon, and time to dry is measured by a stop watch. The critical point is the determination of the dry state of the film. It is often done by touching the film with glass slide<sup>3,7,18</sup> or finger<sup>21</sup> and observing if there are any remains of the liquid on the glass/finger. Another way to detect drying time is creation of the film on the scales and measurement of the weight in prescribed intervals<sup>25</sup>.

For experimental work it's possible to determine the drying time *in vivo* as well, however this method is not suitable for industrial use.

### **1.5.2. Film thickness**

With defined quantity of FFS and application area, film thickness is an accurate and easily measurable parameter. The FFS is applied on the non-sticky surface, usually glass or teflon, and after evaporation of the solvent the formed film is peeled of and thickness is measured with a caliper at multiple locations on one film with subsequent calculation of mean thickness<sup>3,18,20,25</sup>.

### **1.5.3. Tensile strength**

Mechanical properties of the formed film are important to describe its toughness and with that its resistance to the stress caused by skin movements. Texture analyzers enabling the measurement of mechanical characteristics such as breaking strain<sup>25</sup>, maximum force at which

the material stops being elastic and suffers plastic deformation or Young's Modulus<sup>20</sup> are commonly employed.

#### **1.5.4. Film tackiness**

The stickiness of the outer surface of the film is tested by pressing cotton wool on the dry film under low pressure. Depending on the quantity of the fibers retained by the film the tackiness is rated high (dense accumulation of fiber on the film), medium (thin fiber layer on the film) or low (occasional or no adherence of the fibers)<sup>3</sup>.

#### **1.5.5. Water resistance test**

This test is used mostly for nail lacquers. The water resistance test is conducted by applying a nail lacquer onto a substrate, allowing it to dry, then immersing the substrate (with the lacquer film) in water for a defined time, after which the amount of lacquer film lost from the substrate is quantified and visible changes are described<sup>54</sup>.

#### **1.5.6. Gas permeability**

Determination of permeability for natural gases such as oxygen or water vapor is important for prediction of potential occlusive properties of the films which are considered negative. Frequently used methods for measuring of water vapor permeability are set in British Pharmacopoeia<sup>3,18,20</sup> and by ASTM International<sup>55,56</sup>. They are based on determination of weight loss of vial filled with water caused by permeation of water vapor thru the film to the ambient with lower humidity.

#### **1.5.7. Fourier transform infrared analysis**

Fourier transform infrared analysis (FTIR) is used to uncover any possible molecular interactions between drug and polymer. Measurement is commonly performed in the range of 4000 – 400 cm<sup>-1</sup> for formulation with and without drug, consequently these two spectra are compared<sup>21,56,57</sup>.

#### **1.5.8. Thermal analyses**

Differential scanning calorimetry (DSC) and thermogravimetric analysis (TGA) are two most commonly used methods for thermal analysis of FFSs. DSC measures of heat absorbed by a material in comparison with reference which enables assessment of parameters such as glass transition temperature ( $T_g$ ) or melting temperature ( $T_m$ )<sup>56</sup>. It is frequently used to determine the efficacy of plasticizers which are known to decrease the  $T_g$ <sup>26</sup>. On the other hand, TGA measures the change in sample mass with increasing temperature and is used to description of materials' thermal stability<sup>56</sup>.

### 1.5.9. Microstructural analysis

Structure of the films can be monitored using scanning electron microscopy (SEM)<sup>20</sup> or atomic force microscopy (AFM)<sup>58</sup>. Both methods result in images capturing the structure of the films which enable description of the roughness or smoothness of the film and occurrence of other structural features such as pores<sup>20,58</sup>.

### 1.5.10. Drug release

For an evaluation of drug release, Franz diffusion cell and its modifications<sup>3,7,18,20,21</sup> (**Figure 3**) is the most common instrument selected for *in vitro* studies. The FFS is applied on the diffusion membrane clamped between the receptor and donor compartment. Membrane can be made of different materials such as silicone<sup>3</sup>, nylon<sup>7,20</sup> or cellulose<sup>21</sup>. Receptor compartment is filled with chosen receptor phase and tempered to a defined temperature. Release testing is conducted during a given period of time when samples are drawn at predetermined intervals and replaced by aliquots of receptor fluid. The content of drug substance in samples is then determined by a suitable method, for example HPLC or spectrophotometric analysis<sup>3</sup>.

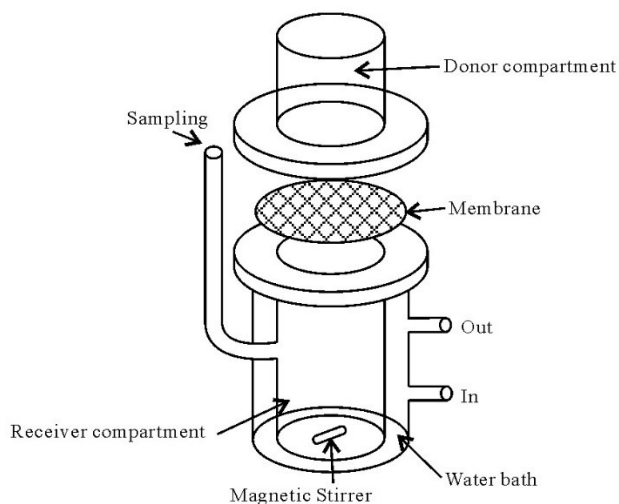


**Figure 3** Scheme of diffusion cell used for *in vitro* drug release testing<sup>59</sup>

### 1.5.11. Rheological characterization

The description of rheological properties of FFSs is very important for understanding of their behavior during development, processing and end use. The rheological characteristics significantly influence not only manufacturing, packaging and stability of FFSs or resulting *in situ* films but also the application which has impact on accuracy of dosing and patients' compliance<sup>60</sup>. Rotational and oscillation tests are commonly employed to describe the rheological behavior of FFS. Rotational (shear) testing is performed to determine flow behavior as a typical characteristic of liquid like materials whereas oscillation tests enable determination of viscoelastic behavior. These are then used to identify the prevailing nature of the system<sup>61</sup>.

## 1.6. Adhesive properties

Adhesion is one of the critical parameters for FFSs. It is necessary for them to form a film with sufficient adhesion to the skin to guarantee continuous delivery of the drug. However, it should not adhere to other materials such as textile to avoid adhesion to clothes. To describe adhesive properties *in vitro*, measurements of tackiness are performed, serving as an objective method for evaluation of adhesive forces between two materials<sup>62</sup>. Although the number of adhesive topical preparations is growing, no method for adhesion strength testing is set in European Pharmacopoeia<sup>63</sup>.

### 1.6.1. Peel off test

A defined volume of FFS is applied on marked area of a glass plate. After the film is formed, it is either cut into squares or left as such and adhesive cellophane tape is applied over its surface and pressed lightly with thumb. Then it's peeled off quickly and area of glass plate containing film residues is calculated and percentage of the area removed by tape is determined<sup>29,57,64</sup>.

### 1.6.2. Tensile tests

Probe tack test was developed to replace the commonly used thumb tack test based on pressing a thumb against the adhesive surface and feeling the force necessary to separate it, which has several drawback such as subjectivity or the fact that it is poorly quantifiable<sup>63</sup>. Probe-tack test allows obtaining a quantitative and controlled measurement of the stickiness: a flat, solid punch, called probe, is brought into contact with the film deposited on a rigid substrate. The detachment force is then recorded while the probe is being pulled away<sup>19</sup>. Usually, three main parameters are observed: peak detachment force, area under the curve and time for peak force to decay by 90%<sup>62</sup>. Probe tack test can be performed completely *in vitro* with standard probe or in *ex vivo* mode when probe is cover with animal skin<sup>20,65</sup>.

### 1.6.3. In vivo adhesion testing

The assessment of adhesion might be done *in vivo* with volunteers which enables testing on human skin under the most representative conditions<sup>22</sup>. However, there are several disadvantages such as necessary administration connected with informed consent and the fact that results might be distorted by the human factor.

## 1.7. Mathematical models for evaluation of flow behavior

To enable easier analysis of complicated rheological characteristics of real materials, theoretical entities with ideal behavior were defined and described with basic rheological parameters such as stress, strain, strain rate and time for which it is subject to the action of such strain. Although the ideal body is an extreme case which the real materials can only bear more or less resemblance to, it allows creation of simplified mathematical models. These are based on relatively small number of fitting parameters and can be used for description of flow curve course facilitating the prediction of rheological behavior at unmeasured regions<sup>66</sup>.

One of the most important rheological characteristics of fluids is their viscosity defined as inner friction that occurs in the liquids during a shear flow. Its dependency on the shear rate plotted in a chart is called viscosity curve while graphical display of relationship between shear stress and shear rate is described as flow curve. Equation for determination of viscosity will be demonstrated for chosen mathematical models<sup>66,67</sup>. For mathematical description of viscosity and flow curves different models are employed depending on the course of the curve and region which needs to be described<sup>68</sup> (**Figure 4**). Suitability of the model is than express by the correlation coefficient.

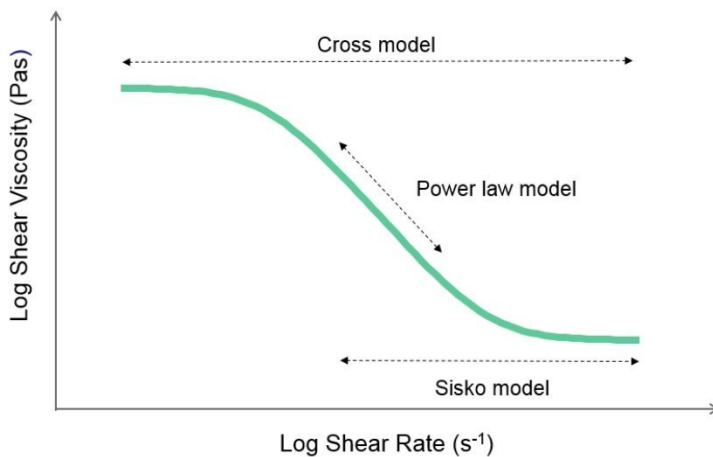


**Figure 4** Viscosity curve and relevant models for description of its course, logarithmic scale <sup>67</sup>

### 1.7.1. Newton model

Newtonian fluids represent the basic mathematical model for fluids where shear stress is linearly related to the shear rate. This means viscosity, calculated as share of shear stress and shear rate, is constant, not depending on the mentioned two measures and thus considered material characteristic. The equation as follows (2)<sup>66</sup>:

$$\eta = \frac{\tau}{\dot{\gamma}} \quad (2)$$

where:

$\eta$  shear viscosity [Pa·s]

$\tau$  shear stress [Pa]

$\dot{\gamma}$  shear rate [s<sup>-1</sup>]

### 1.7.2. Power law model

The most commonly used mathematical model for non-Newtonian fluids is the Power law model created by W. Ostwald and A. de Waele (3). It describes the intermediate (linear) shear rate regions<sup>66</sup> and gives the basic relation between viscosity and shear rate. It contains only two constants that need to be determined<sup>69</sup>:

$$\eta = K\dot{\gamma}^{n-1} \quad (3)$$

where:

$\eta$  shear viscosity [Pa·s]

$K$  consistency index [Pa·s<sup>n</sup>]

$\dot{\gamma}$  shear rate [s<sup>-1</sup>]

$n$  power law index [-]

The power law index defines the slope of the viscosity curve and its values are clearly connected with different types of fluids, resp. their rheological behavior. Fluids with  $n < 1$  have pseudoplastic properties, those with  $n = 1$  are Newtonian and materials whose  $n > 1$  show dilatant behavior. Value of consistency index ( $K$ ) is numerically equal to that of shear viscosity at shear rate of 1 s<sup>-1</sup> (<sup>69,70</sup>).

### 1.7.3. Sisko model

Sisko flow equation was first introduced in 1958 by A.W. Sisko to describe the flow of lubricating greases in the wider range of shear rates and is still frequently used especially for calculation of rheological parameters of shear thinning fluid at high shear rates<sup>66,71</sup>. Calculation of shear viscosity according to this model is carried out using the equation (4)<sup>72</sup>.

$$\eta = \eta_{\infty} + K\dot{\gamma}^{n-1} \quad (4)$$

where

$\eta$  shear viscosity [Pa·s]

$\eta_{\infty}$  infinite-shear-rate viscosity [Pa·s]

$\dot{\gamma}$  shear rate [s<sup>-1</sup>]

$K$  consistency index [Pa·s<sup>n</sup>]

$n$  empirically determined index exponent, so called power law index, dimensionless



#### 1.7.4. Cross model

This model is used to investigate the behavior of shear thinning fluids in the whole range of shear rates covering zero shear and infinite shear plateaus as well. Even though the materials are considered shear thinning they might show Newtonian properties (constant viscosity) in these regions. Cross model belongs to the most popular models employed in viscosity data analysis today, expressing shear viscosity as follows (5):<sup>72</sup>

$$\eta = \eta_{\infty} + \frac{\eta_0 - \eta_{\infty}}{1 + (C\dot{\gamma})^m} \quad (5)$$

where

$\eta$  shear viscosity [Pa·s]

$\eta_{\infty}$  infinite-shear-rate viscosity [Pa·s]

$\eta_0$  zero-shear-rate viscosity [Pa·s]

$\dot{\gamma}$  shear rate [ $s^{-1}$ ]

C empirically determined constant, so called Cross constant [s]

m empirically determined exponent, so called shear thinning or Cross index, dimensionless

Considering the value of shear viscosity is much lower than the zero-shear-rate viscosity and concurrently much higher than infinite-shear-rate viscosity, this model can be reduced to the previously mentioned Power law model. Besides that, the shear thinning index (m) ranging from 0 (Newtonian) to 1 (infinitely shear thinning) correlates with power law index (n) according to the following equation (6)<sup>67</sup>:

$$n = 1 - m \quad (6)$$

## **2 EXPERIMENTAL PART**

### **2.1. Materials**

#### **2.1.1. Substances**

Aceton p.a. (Lachema a.s.), CAS: 67-64-1

Ethanol 96% (Penta Chrudim), CAS: 64-17-5

Ethyl pyruvate (Sigma- Aldrich), CAS: 617-35-6

Methyl salicylate (Sigma- Aldrich), CAS: 119-36-8

Phosphate buffer tablets (Sigma- Aldrich)

Polymer PLGA (Department of Pharmaceutical technology, FaF UK HK)

Polymer 2A (Department of Pharmaceutical technology, FaF UK HK)

Polymer 8D (Department of Pharmaceutical technology, FaF UK HK)

Polymer 3T (Department of Pharmaceutical technology, FaF UK HK)

Purified water (FaF UK HK), CAS: 7732-18-5

Salicylic acid (Fagron a.s.), CAS: 69-72-7

Triacetin (Sigma- Aldrich), CAS: 102-76-1

#### **2.1.2. Devices**

Alu crucibles + lids, NETSCH

Analytical digital scales KERN<sup>®</sup> ABS, max. 220 g, d=0,001 g, Fisher Scientific

Analytical digital scales KERN<sup>®</sup> FKB, max. 8100 g, d=0,05 g, Fisher Scientific

Microbalance analytical scale CAHN 26, CAHN Instruments

Heat- flux DSC 200 F3 Maia<sup>®</sup>, NETSCH

Drying oven MEMMERT<sup>®</sup> ULE 400

Rotational rheometer Kinexus Pro+, Malvern Instruments

Shaking water bath Julabo SW22, Fisher Scientific

Spectrophotometer Specord 205, Analytik Jena

## 2.2. DSC

Thermal analysis of polymers PLGA, 2A, 8D and 3T as well as of the salicylic acid loaded polymer 2A plasticized with EP was performed with Heat- flux DSC 200 F3 Maia<sup>®</sup> from NETSCH and its accessories. Samples of tested materials were weighted on the CAHN 26 analytical scales in the aluminium crucibles with volume of 25  $\mu$ l, closed with the aluminium lids and hermetically sealed using special press. The quantity of samples ranged from 4 to 6 mg. The sample and reference crucible were positioned on the separate temperature sensors and the cell was closed. The operating software DSC 200F3 was launched and weights of sample, sample crucible and reference crucible were entered, followed by the setup of temperature regime. Then the test was initiated. The temperature range was chosen according to the melting point of the drug and the expected values of  $T_g$  of the polymeric carriers. Complete temperature scheme is mentioned in the **Figure 5**. Analysis of the obtained results was performed in the software Proteus<sup>®</sup>. The  $T_g$  was determined in the inflection point of the second heating DSC curve as average of the three measurements with a standard deviation.

Num	Mode	°C	K/min	pts/min	hh:mm	STC	Co
● ---	Initial	22.0				1	1
➡ 1	Isothermal	22.0		50.00	00:05	1	1
↙ 2	Dynamic	-20.0	10.000	300.00	00:04	1	1
➡ 3	Isothermal	-20.0		50.00	00:05	1	1
↗ 4	Dynamic	180.0	10.000	300.00	00:20	1	1
➡ 5	Isothermal	180.0		150.00	00:02	1	1
↙ 6	Dynamic	-20.0	10.000	300.00	00:20	1	1
➡ 7	Isothermal	-20.0		50.00	00:05	1	1
↗ 8	Dynamic	180.0	10.000	600.00	00:20	1	1
↙ 9	Dynamic	20.0	10.000	600.00	00:16	1	1
⊕ 10	Emergency	190.0					0
F ---	StdBy Heat.	20.0	20.000		00:00	1	1
E ---	StdBy Iso	20.0			00:20	1	0

*Figure 5 Temperature regime of DSC.*

## 2.3. Rheological testing

Measurement of rheological behavior of PLGA, 2A, 3T and 8D plasticized with different plasticizers or different concentrations of the same plasticizer was performed using a rotary rheometer KinexusPro<sup>+</sup> by Malvern, powered by software rSpace. Before switching the device on, the supply of compressed air was checked and all covers were removed. The 5 minutes initial stabilization of the rheometer was followed by the launch of the software. After the consequent device-software communication check the measurements were initiated, following

exact instructions of the software. For all tests the geometry PU 20 (upper plate 20 mm) in combination with solvent trap was employed. Test conditions were chosen based on the test to be performed and sample characteristics.

### 2.3.1. Rotation testing

Shear viscosity of the PLGA, 2A and 3T polymers plasticized with 30% of EP, MS or TA at 25 °C, 37 °C or 50 °C, 8D plasticized with MS at concentrations of 10%, 20% or 30% at 25 °C, 37 °C or 50 °C and 3T plasticized with EP at concentrations of 10%, 20%, 30% or 40% at 37 °C was tested using the sequence *Toolkit\_V005 Shear Rate Ramp – Alternative Flow Curve (V005)*, input parameters are summarized in the **Table 5**. For evaluation of the flow curve analysis sequences *Analyse\_0004 Power law model fit for viscometry* and *Analyse\_0021 Newtonian model fit for viscometry* were employed. Data are presented as means ± standard error of mean, n = 3.

**Table 5** Set up parameters used for sequence shear rate ramp

Shear rate range	Samples per decade	Working gap	Temperature
0.1 – 100.0 s <sup>-1</sup>	10	0.2 mm	25 °C
			37 °C
			50 °C

### 2.3.2. Oscillation testing

For determination of viscous and elastic moduli and phase angle of 3T plasticized with 30% of EP, MS or TA at 25 °C and 8D plasticized with MS at concentrations of 10%, 20% or 30% at 25 °C sequence *Oscillation\_0004 Amplitude sweep shear strain controlled with LVER determination* was used. To additionally test the temperature dependency of these two characteristics of 3T plasticized with 30% of TA sequence *Measure\_0029 Single frequency strain controlled temperature ramp* was employed. In the first mentioned temperature is constant whereas it is being increased in the given range during the second test. Data are presented as means ± standard error of mean, n = 3.

**Table 6** Set up parameters used for oscillation tests

Sequence	Shear strain range	Samples per decade	Working gap	Temperature	Frequency
<i>Oscillation_0004</i>	0.01 – 100%	10	1.0 mm	25 °C	1 Hz
<i>Measure_0029</i>				25 – 95 °C	

## 2.4. Adhesion

Adhesive properties of PLGA, 2A and 3T polymers plasticized with 30% of EP, MS or TA at 25 °C and 8D plasticized with MS at concentrations of 10%, 20% or 30% at 25 °C were measured using rotational rheometer and the predefined sequence rSolution\_0020 Evaluating tackiness and adhesion using a pull away test (rS\_0020). Input parameters are summarized below (**Table 7**). Adhesion was expressed as the peak detachment force and time necessary to decrease the force by 90% of the five measurements with standard deviation. Data are presented as means  $\pm$  standard error of mean, n = 5.

*Table 7 Set up parameters used for adhesion test*

Working gap	Gapping speed	Temperature
0.2 mm	25 mm/s	25 °C

## 2.5. SEM

SEM was performed at Department of Physics, Faculty of Science, University of Hradec Kralove. The microstructure of *in situ* formed films was examined using a scanning electron microscope FlexSEM 1000 (Hitachi, Japan) at accelerating voltages of 15 kV and 20 kV. Before the measurement, the samples were coated with 8 nm thick golden layer by EM ACE200 sputter coater (Leica, Germany). The film made of polymer 2A loaded with 5% of salicylic acid without a plasticizer or plasticized with 30% of methyl salicylate was tested. The top surfaces and the fracture surfaces of the films were observed.

## 2.6. FFS formulation

FFS solutions were prepared by dissolving the given amount of PLGA derivative and drug in acetone, and finally adding methyl salicylate. Amount of acetone used was equivalent to the total weight of other constituents. Composition of all prepared variants is summarized in the **Table 8**. After incorporation of plasticizer the mixture was kept in closed vials at the room temperature on the magnetic stirrer until complete dissolution.

**Table 8** Composition of salicylates loaded PLGA-based FFS.

<b>Formulation</b>	<b>Polymer 2A</b>	<b>Drug Salicylic acid</b>	<b>Plasticizer Methyl salicylate</b>	<b>Solvent Aceton</b>
FFS 1	1700 mg	100 mg	200 mg	2000 mg
FFS 2	1800 mg	200 mg	200 mg	2000 mg
FFS 3	1500 mg	100 mg	400 mg	2000 mg

## 2.7. Drug release

An amount of 500  $\mu$ l of all FFSs prepared according to 2.6 was pipetted into glass vial and left to dry under ambient conditions. Weight of dried films was noted to enable calculation of total amount of salicylates. Dissolution test was performed in shaking water bath under 37 °C, dried films were poured over with 10 ml of PBS pH 7.4. Samples were withdrawn after 5, 24, 48, 72, 96, 144 and 264 h and replaced with the same volume of fresh PBS. Content of salicylates was determined spectrophotometrically using calibration curve (Figure 6) method. From the values of absorbance at 298 nm obtained for each time cumulative percentage of released salicylates was calculated and plotted into a dissolution chart. Testing was performed in triplicate for each FFS with subsequent calculation of average content of released salicylates.

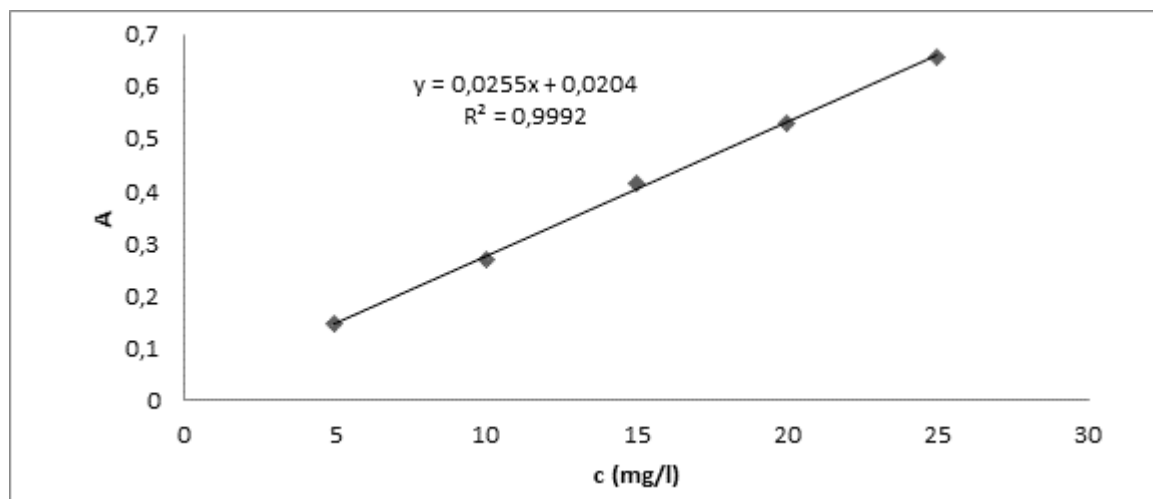


**Figure 6** Calibration curve of salicylic acid<sup>73</sup>

### 3 RESULTS

#### 3.1. DSC

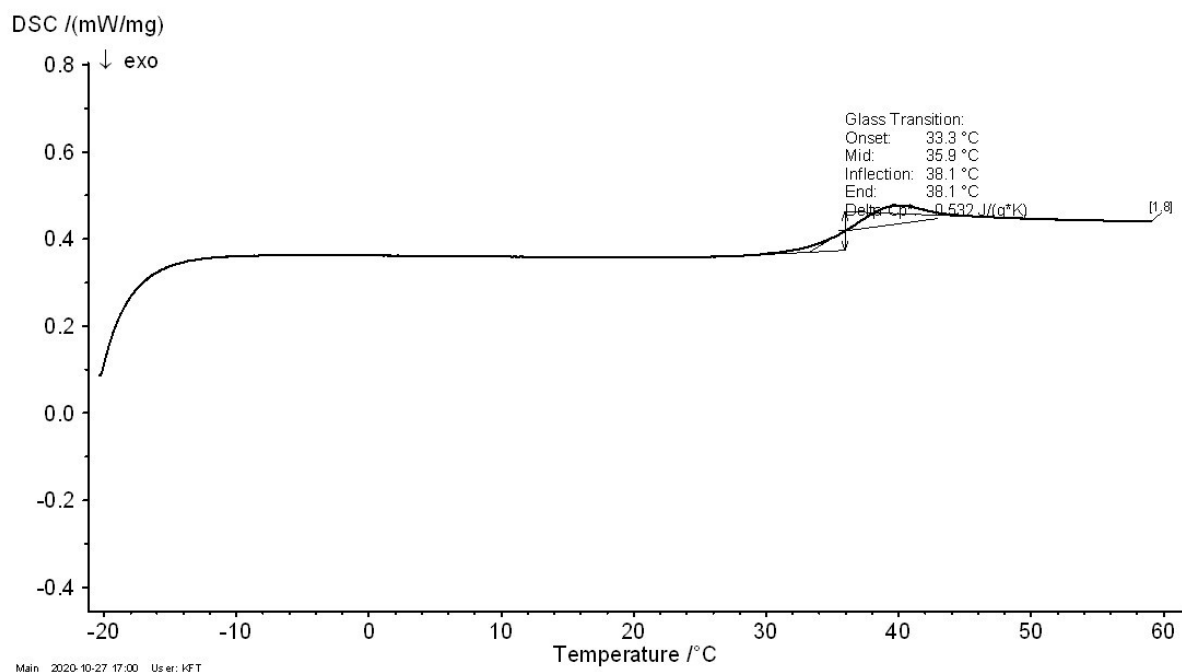


Figure 7 DSC record of linear polymer PLGA.

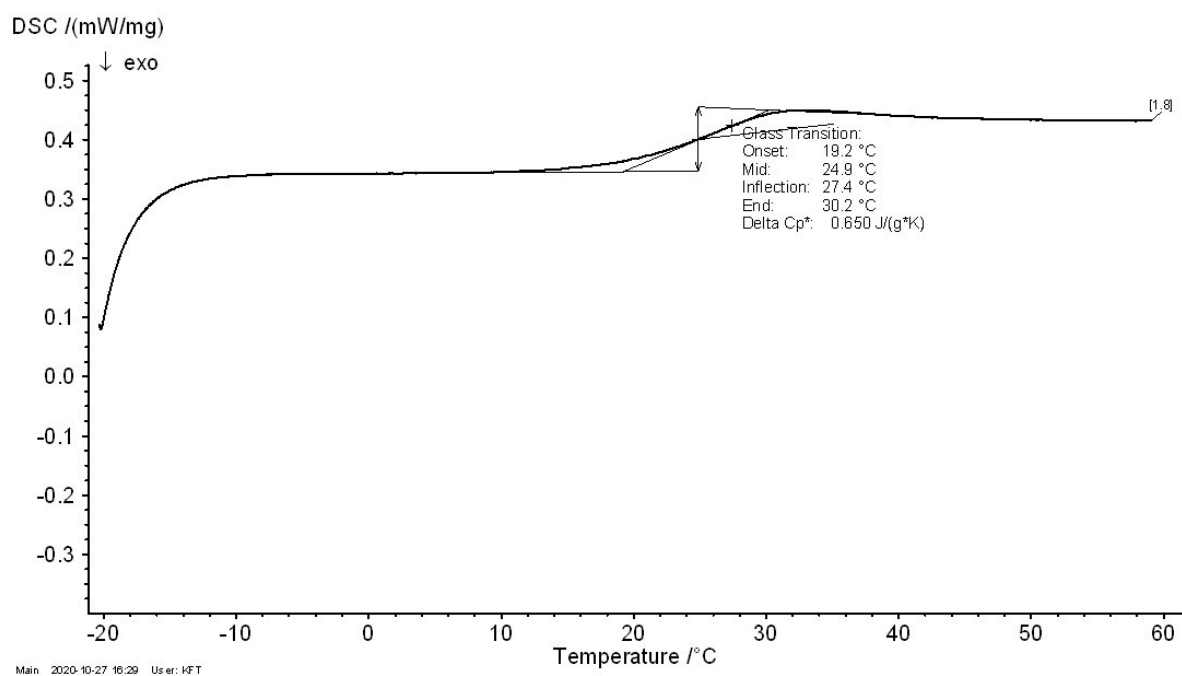
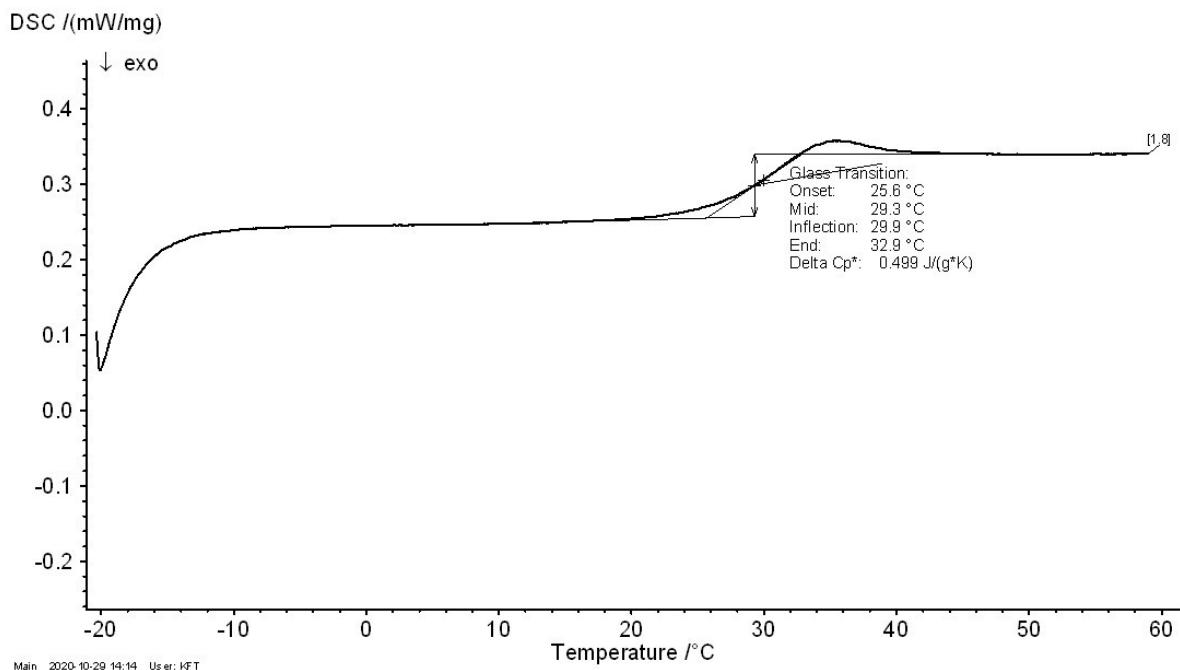
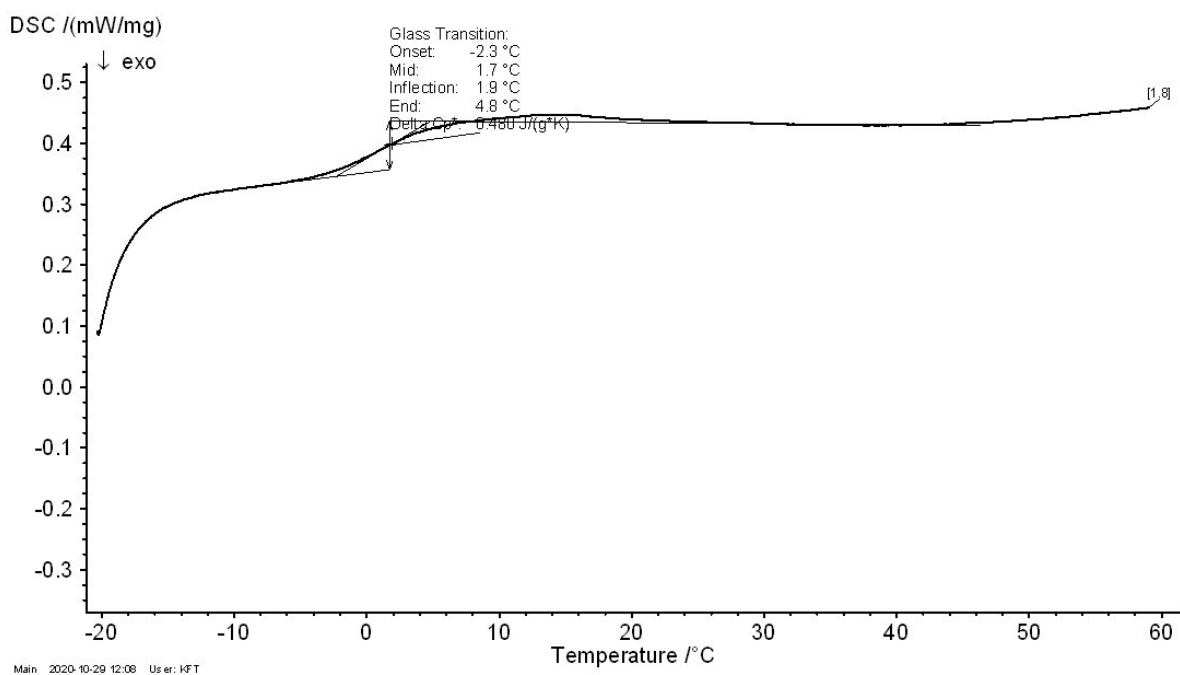


Figure 8 DSC record of branched polymer 2A.



**Figure 9** DSC record of branched polymer 3T.



**Figure 10** DSC record of branched polymer 8D.



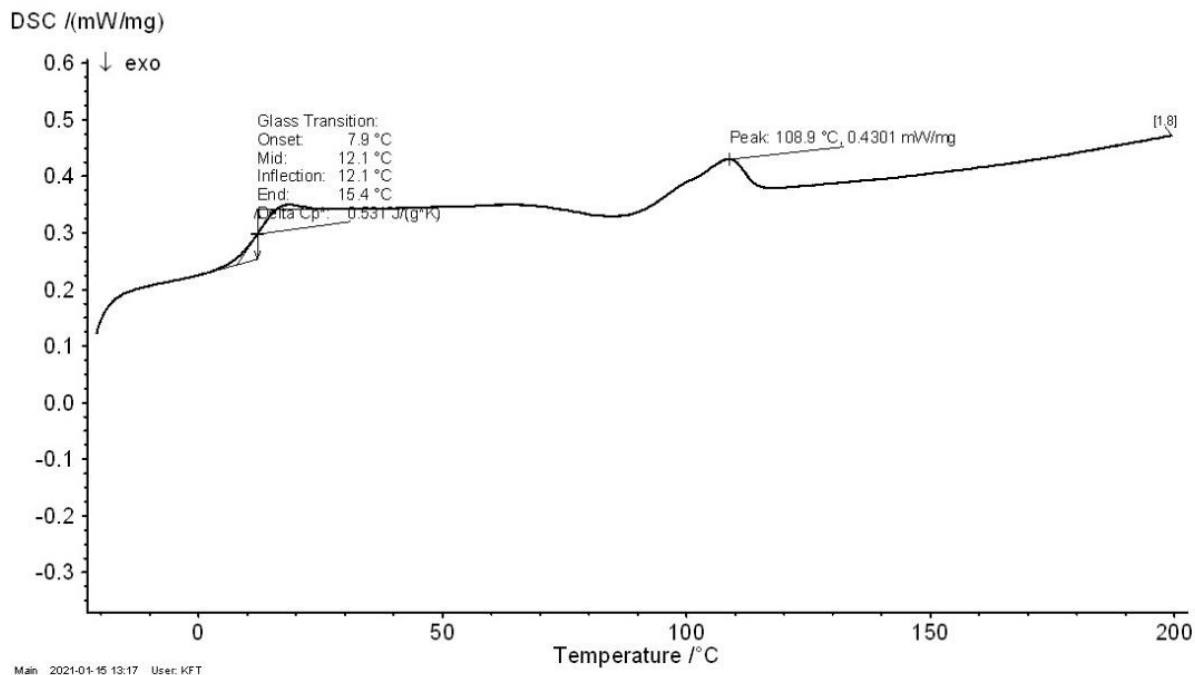


**Figure 11** DSC record of salicylic acid (20%) loaded branched polymer 2A.

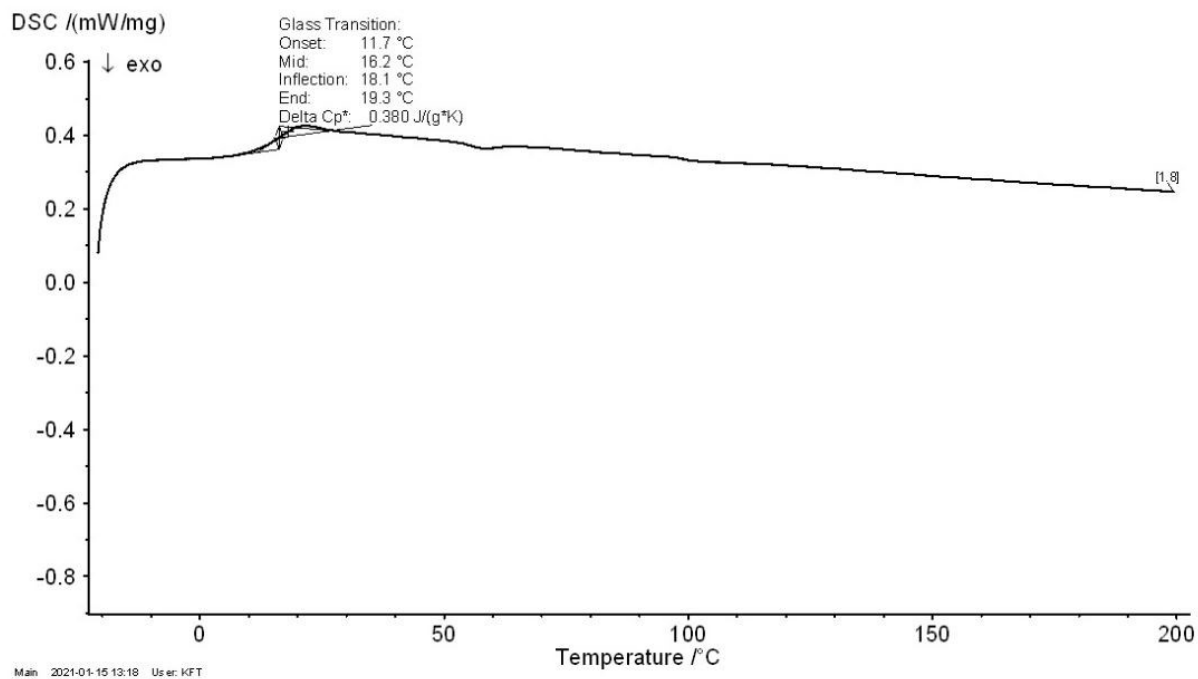


**Figure 12** DSC record of salicylic acid (5%) loaded branched polymer 2A plasticized with 10% of EP.

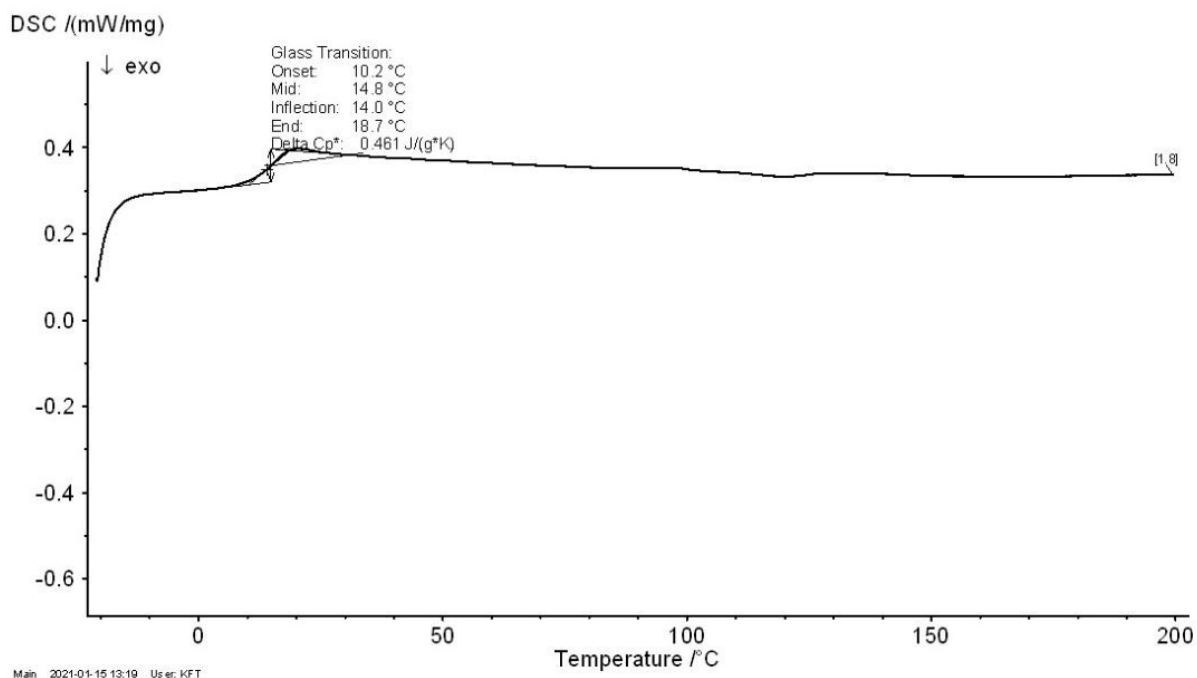


**Figure 13** DSC record of salicylic acid (10%) loaded branched polymer 2A plasticized with 10% of EP.

**Table 9** Glass transition temperatures of tested polymers determined by DSC.

Polymer	T <sub>g</sub> (°C) ± SD
PLGA	38.1 ± 1.8
2A	27.4 ± 1.5
3T	29.9 ± 1.6
8D	1.9 ± 0.1
2A + 20% SA	12.1 ± 0.5
2A + 5% SA + 10% EP	18.1 ± 0.7
2A + 10% SA + 10% EP	14.0 ± 0.7

## 3.2. Rheological characterization

### 3.2.1. Viscosity curves

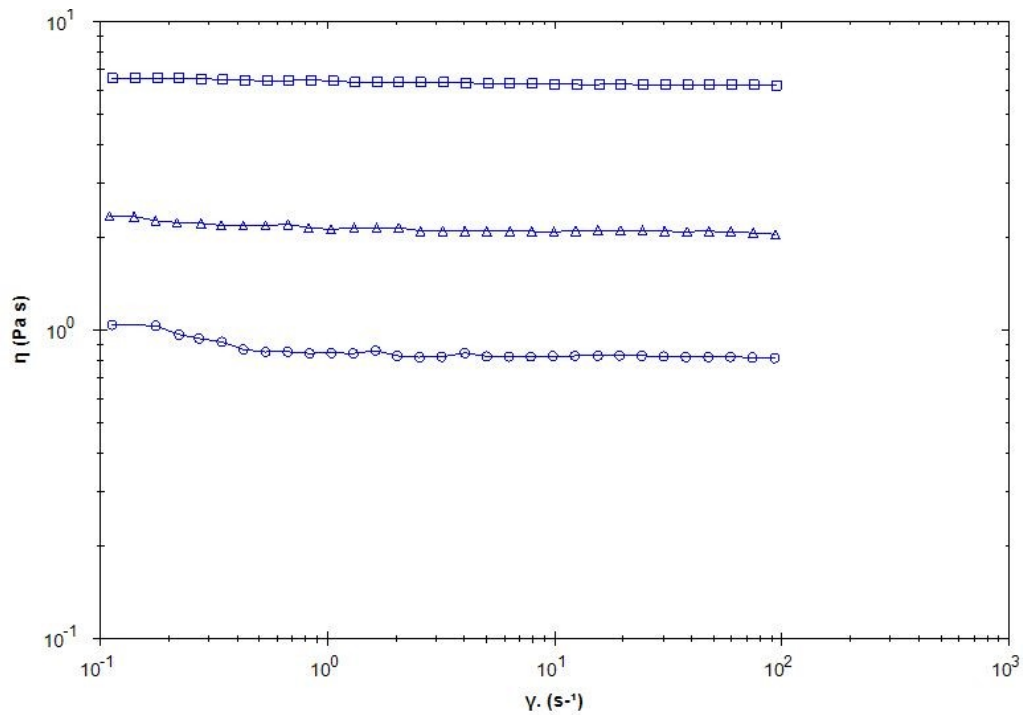


**Figure 14** Viscosity curves of PLGA plasticized with 30% of EP at different temperatures: 25 °C (squares), 37 °C (triangles), 50 °C (circles)

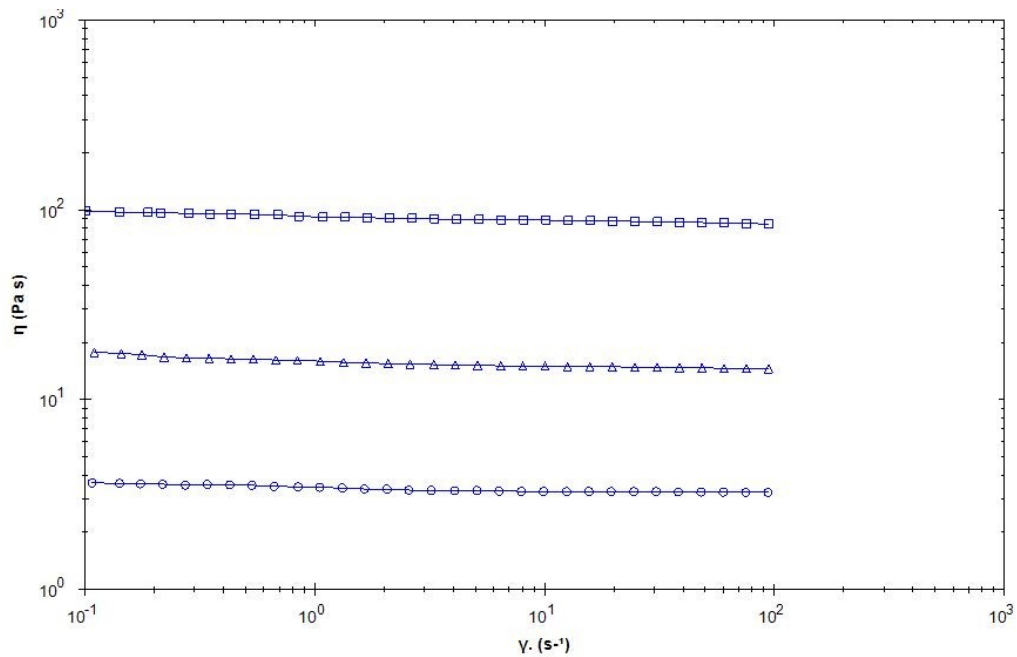


**Figure 15** Viscosity curves of PLGA plasticized with 30% of MS at different temperatures: 25 °C (squares), 37 °C (triangles), 50 °C (circles)

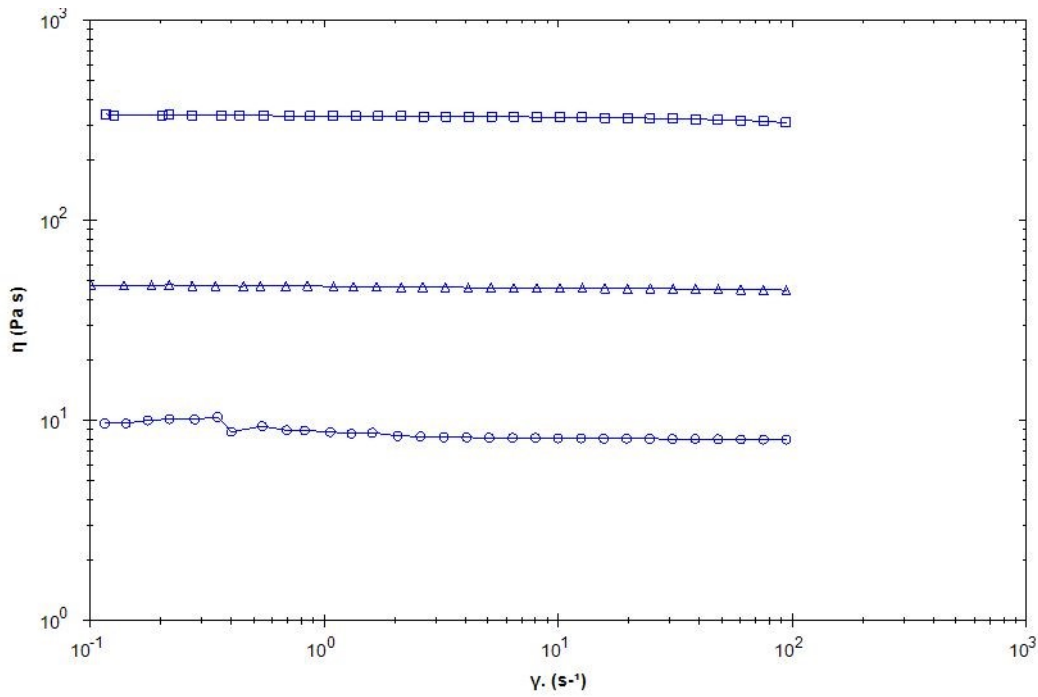


**Figure 16** Viscosity curves of PLGA plasticized with 30% of TA at different temperatures: 25 °C (squares), 37 °C (triangles), 50 °C (circles)

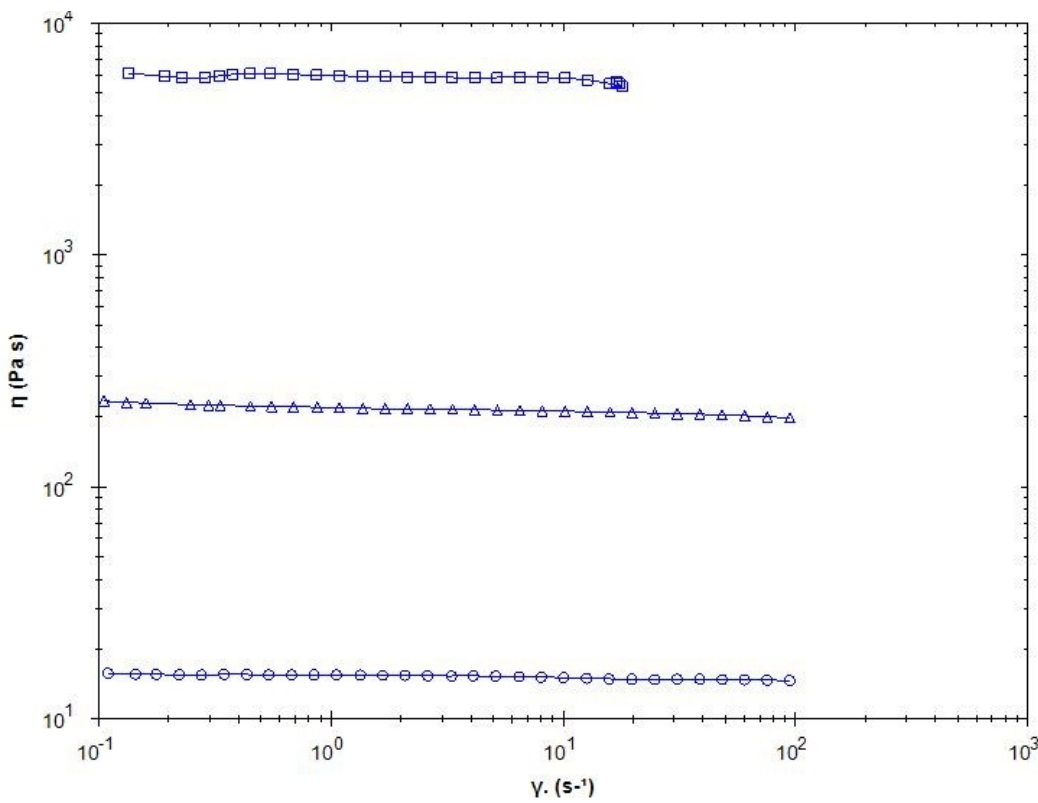


**Figure 17** Viscosity curves of branched polymer 8D plasticized with 10% (squares), 20% (triangles) and 30% (circles) of MS at 25 °C.

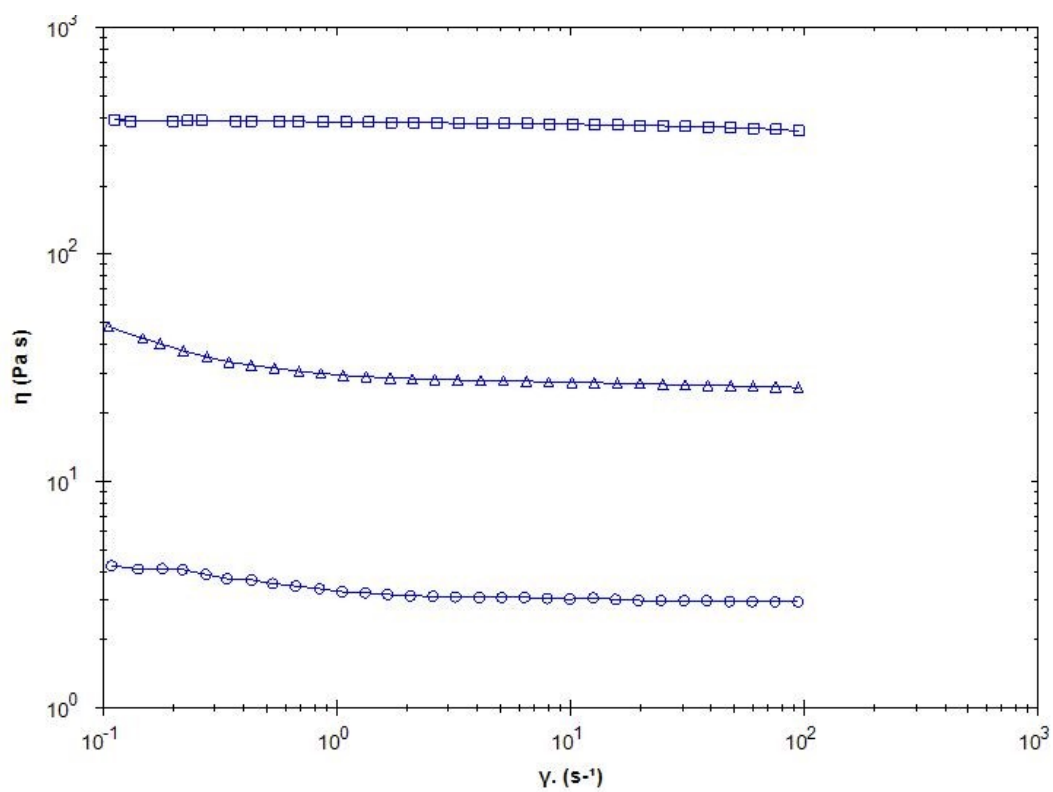


**Figure 18** Viscosity curves of branched polymer 8D plasticized with 10% (squares), 20% (triangles) and 30% (circles) of MS at 37 °C.

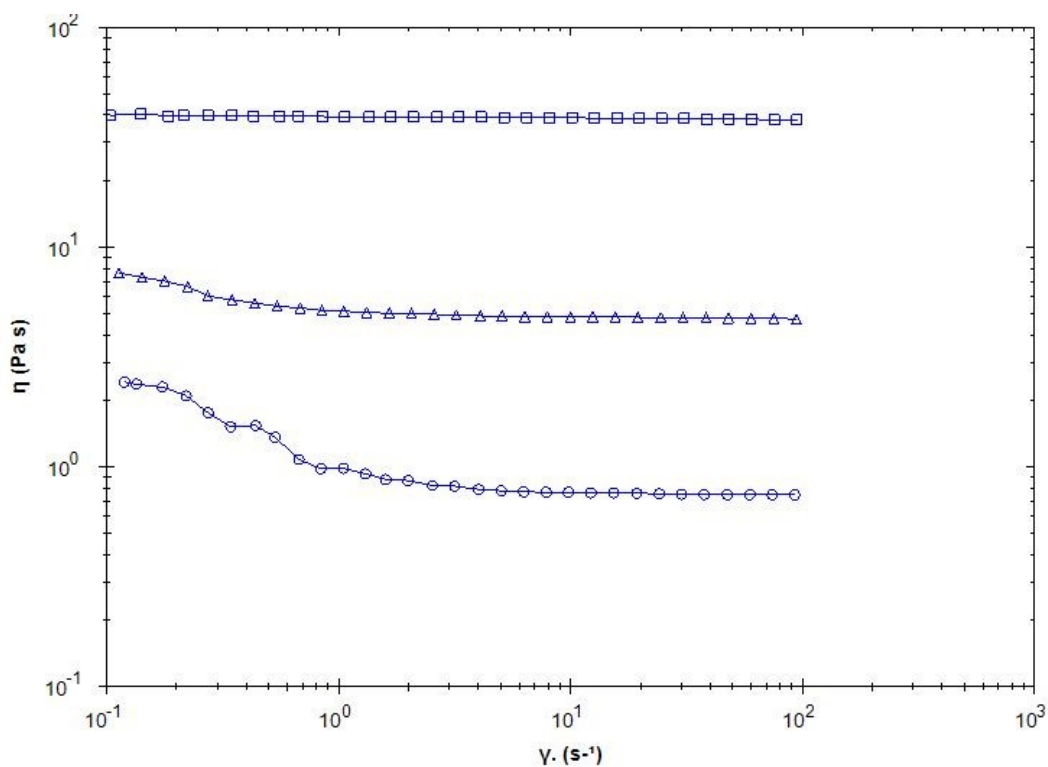


**Figure 19** Viscosity curves of branched polymer 8D plasticized with 10% (squares), 20% (triangles) and 30% (circles) of MS at 50 °C.

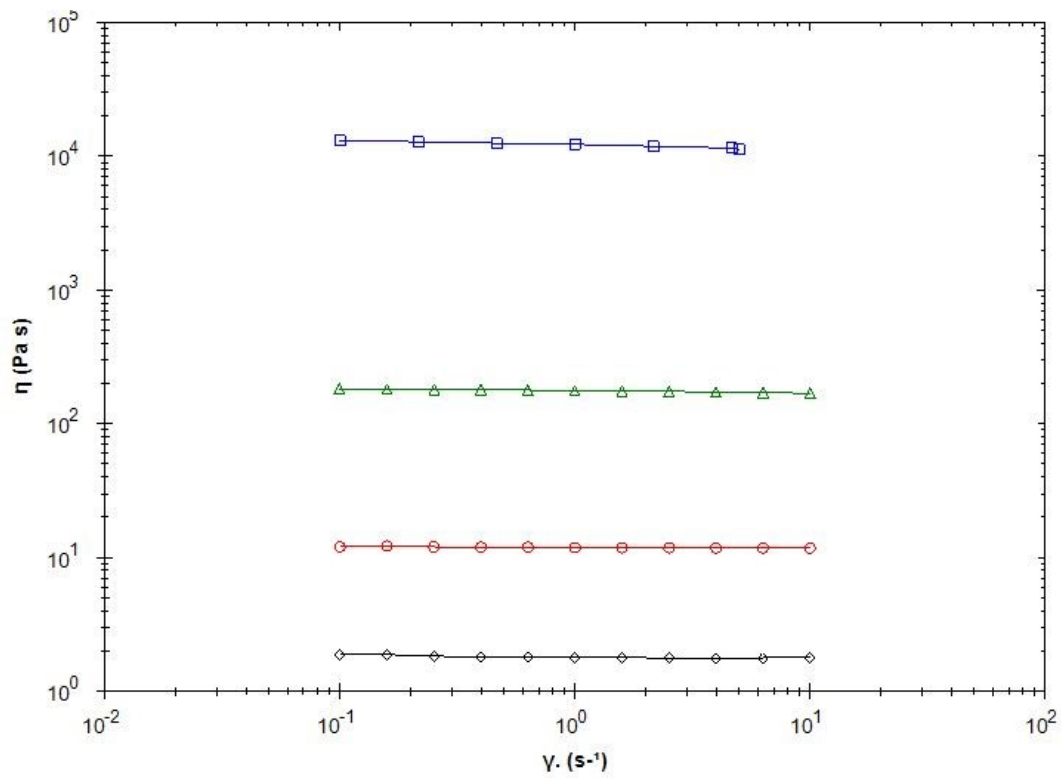


**Figure 20** Viscosity curves of branched polymer 3T plasticized with 10% (blue), 20% (green), 30% (red) and 40% (black) of EP at 37 °C.

### 3.2.2. Values of consistency index, power law index a shear viscosity

**Table 10** Values of Power law coefficients and shear viscosity (Newton model) of PLGA plasticized with 30% of EP, MS and TA for different temperatures.

Temperature	Sample composition	Power law			Newton	
		K (Pa·s <sup>n</sup> )	n (-)	corr.	η (Pa·s)	corr.
25 °C	PLGA + 30% EP	6.425	0.992	1.0000	6.247	1.0000
	PLGA + 30% MS	92.89	0.978	1.0000	86.01	0.9999
	PLGA + 30% TA	332.0	0.990	1.0000	317.3	0.9998
37 °C	PLGA + 30% EP	2.177	0.985	1.0000	2.080	0.9999
	PLGA + 30% MS	16.09	0.973	1.0000	14.75	1.0000
	PLGA + 30% TA	46.67	0.992	1.0000	45.24	1.0000
50 °C	PLGA + 30% EP	0.882	0.974	0.9997	0.820	1.0000
	PLGA + 30% MS	3.460	0.982	1.0000	3.266	1.0000
	PLGA + 30% TA	8.996	0.964	0.9998	8.074	1.0000

**Table 11** Values of Power law coefficients and shear viscosity (Newton model) of 2A plasticized with 30% of EP, MS and TA for different temperatures.

Temperature	Sample composition	Power law			Newton	
		K (Pa·s <sup>n</sup> )	n (-)	corr.	η (Pa·s)	corr.
25 °C	2A + 30% EP	13.50	0.988	1.0000	12.88	0.9999
	2A + 30% MS	304.9	0.980	1.0000	280.6	0.9996
	2A + 30% TA	1049	0.969	0.9995	897.6	0.9885
37 °C	2A + 30% EP	5.048	0.973	0.9999	4.484	0.9990
	2A + 30% MS	50.47	0.984	1.0000	47.67	1.0000
	2A + 30% TA	139.7	0.989	1.0000	133.5	0.9999
50 °C	2A + 30% EP	2.357	0.959	0.9996	1.954	0.9957
	2A + 30% MS	10.46	0.989	1.0000	10.05	1.0000
	2A + 30% TA	23.46	0.994	1.0000	22.97	1.0000

**Table 12** Values of Power law coefficients and shear viscosity (Newton model) of 3T plasticized with 30% of EP, MS and TA for different temperatures.

Temperature	Sample composition	Power law			Newton	
		K (Pa·s <sup>n</sup> )	n (-)	corr.	η (Pa·s)	corr.
25 °C	3T + 30% EP	22.86	0.996	1.0000	22.37	1.0000
	3T + 30% MS	267.6	0.982	1.0000	248.3	0.9997
	3T + 30% TA	985.8	0.967	0.9997	837.7	0.9910
37 °C	3T + 30% EP	7.268	0.987	0.9999	6.768	0.9995
	3T + 30% MS	46.90	0.977	1.0000	43.51	1.0000
	3T + 30% TA	138.9	0.989	1.0000	132.7	0.9999
50 °C	3T + 30% EP	2.824	0.961	0.9998	2.481	0.9995
	3T + 30% MS	9.905	0.984	1.0000	9.447	1.0000
	3T + 30% TA	24.70	0.997	1.0000	24.40	1.0000

**Table 13** Values of Power law coefficients and shear viscosity (Newton model) of 8D plasticized with 10, 20 and 30% of MS for different temperatures.

Temperature	Sample composition	Power law			Newton	
		K (Pa·s <sup>n</sup> )	n (-)	corr.	η (Pa·s)	corr.
25 °C	8D + 10% MS	5883	0.981	0.9999	5572	0.9989
	8D + 20% MS	221.1	0.980	1.0000	204.8	0.9999
	8D + 30% MS	15.39	0.990	1.0000	14.79	1.0000
37 °C	8D + 10% MS	382.3	0.987	1.0000	361.2	0.9998
	8D + 20% MS	32.20	0.934	0.9991	26.47	0.9999
	8D + 30% MS	3.475	0.948	0.9997	2.972	1.0000
50 °C	8D + 10% MS	39.44	0.993	1.0000	38.39	1.0000
	8D + 20% MS	5.585	0.945	0.9992	4.780	1.0000
	8D + 30% MS	1.230	0.829	0.9931	0.759	1.0000

**Table 14** Values of Power law coefficients and shear viscosity (Newton model) of 3T plasticized with 10, 20, 30 and 40% of MS at 37 °C.

Temperature	Sample composition	Power law			Newton	
		K (Pa·s <sup>n</sup> )	n (-)	corr.	η (Pa·s)	corr.
37 °C	3T + 10% EP	12 140	0.963	1.0000	11 290	0.9997
	3T + 20% EP	176.6	0.984	1.0000	169.2	0.9999
	3T + 30% EP	11.91	0.994	1.0000	11.78	1.0000
	3T + 40% EP	1.808	0.988	1.0000	1.778	1.0000



### 3.2.3. Oscillation

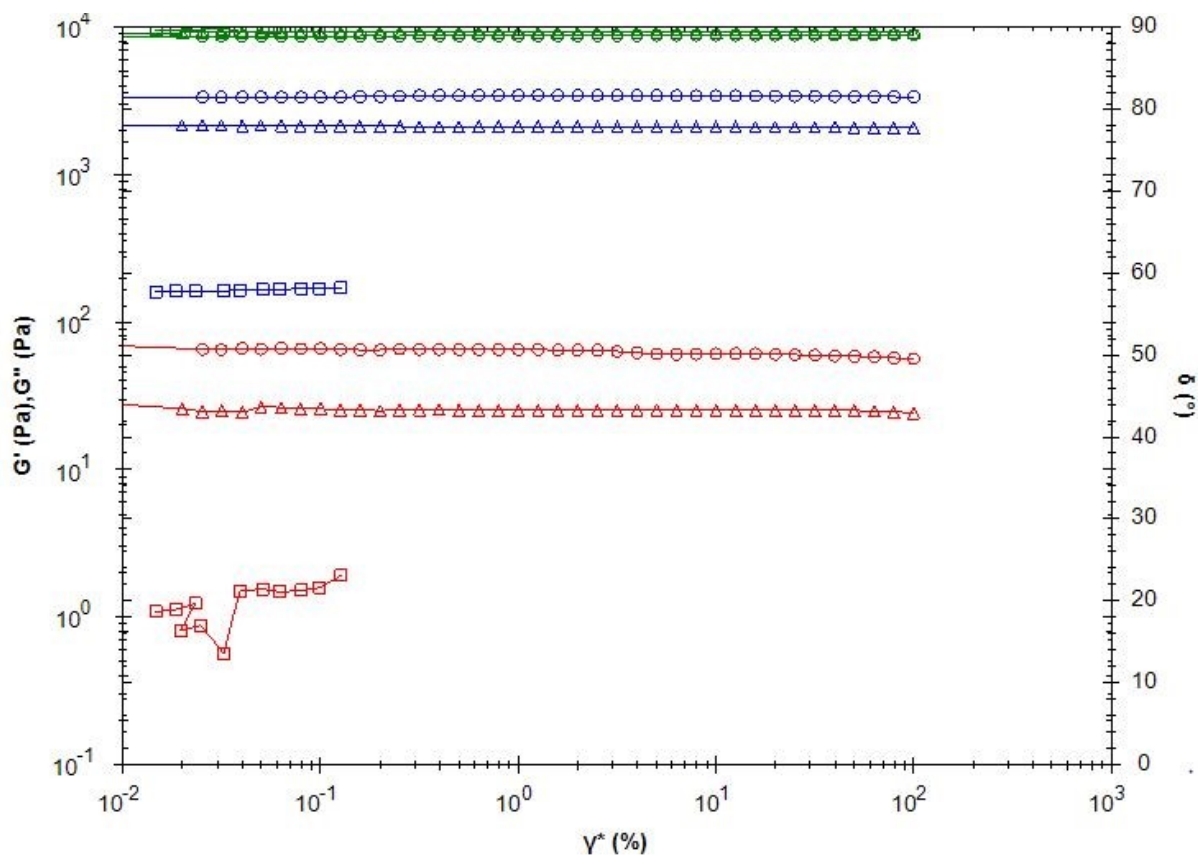


**Figure 21** Elastic modulus  $G'$  (red), viscous modulus  $G''$  (blue), and phase angle  $\delta$  (green) of 3T plasticized with 30% of EP (squares), MS (triangles) and TA (circles) at 25 °C.

**Table 15** Values of elastic modulus ( $G'$ ), viscous modulus ( $G''$ ), and phase angle ( $\delta$ ) of 3T polymer plasticized with different plasticizers at 25 °C.

Sample	$G'$ (Pa)	$G''$ (Pa)	$\delta$ (°)
3T + 30% EP	1.27	165	90
3T + 30% MS	25	2121	89
3T + 30% TA	66	3405	89

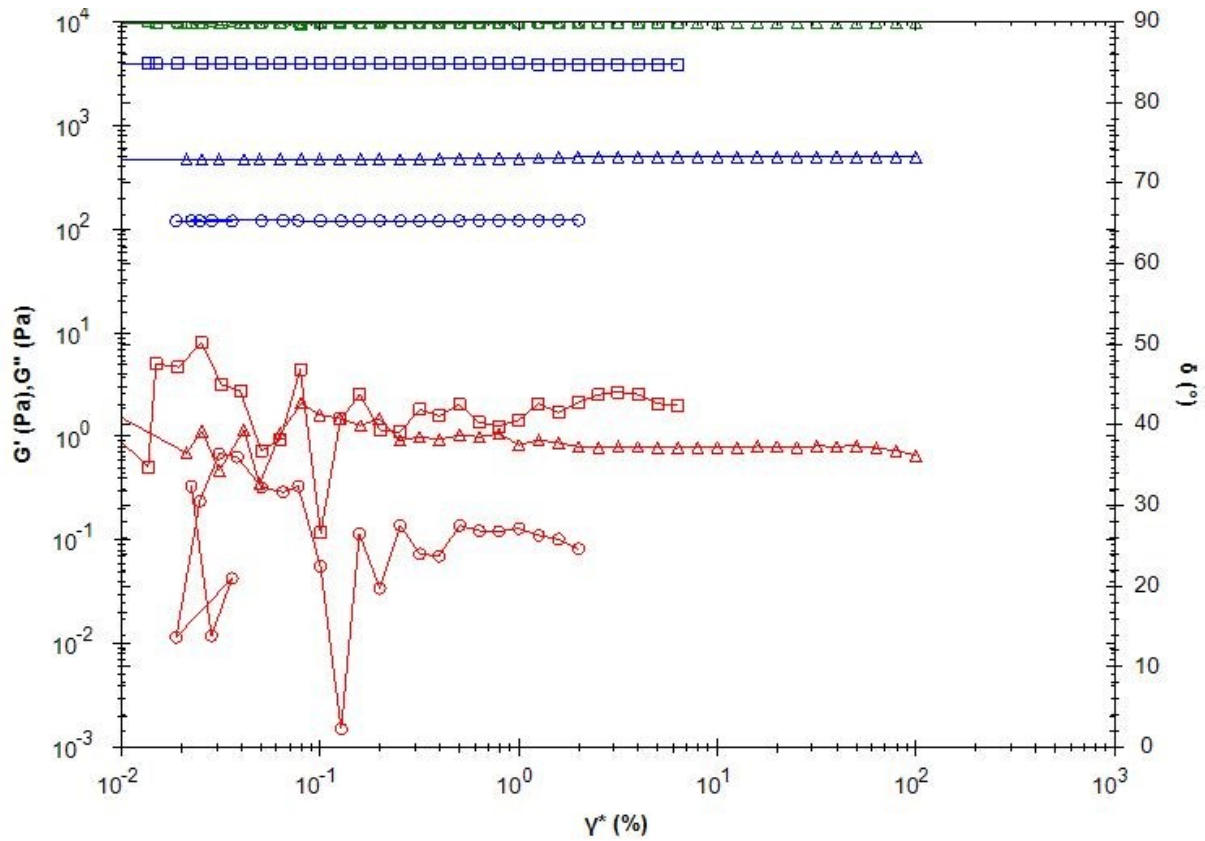


**Figure 22** Viscous modulus (blue), elastic modulus (red) and phase angle (green) of 8D plasticized with 10 (squares), 20 (triangles) and 30 (circles) % of MS at 25 °C.

**Table 16** Values of elastic modulus ( $G'$ ), viscous modulus ( $G''$ ), and phase angle ( $\delta$ ) of 8D polymer plasticized with MS at 25 °C.

Sample	$G'$ (Pa)	$G''$ (Pa)	$\delta$ (°)
8D + 10% MS	2.24	3935	90
8D + 20% MS	1.02	485	90
8D + 30% MS	0.17	121	90

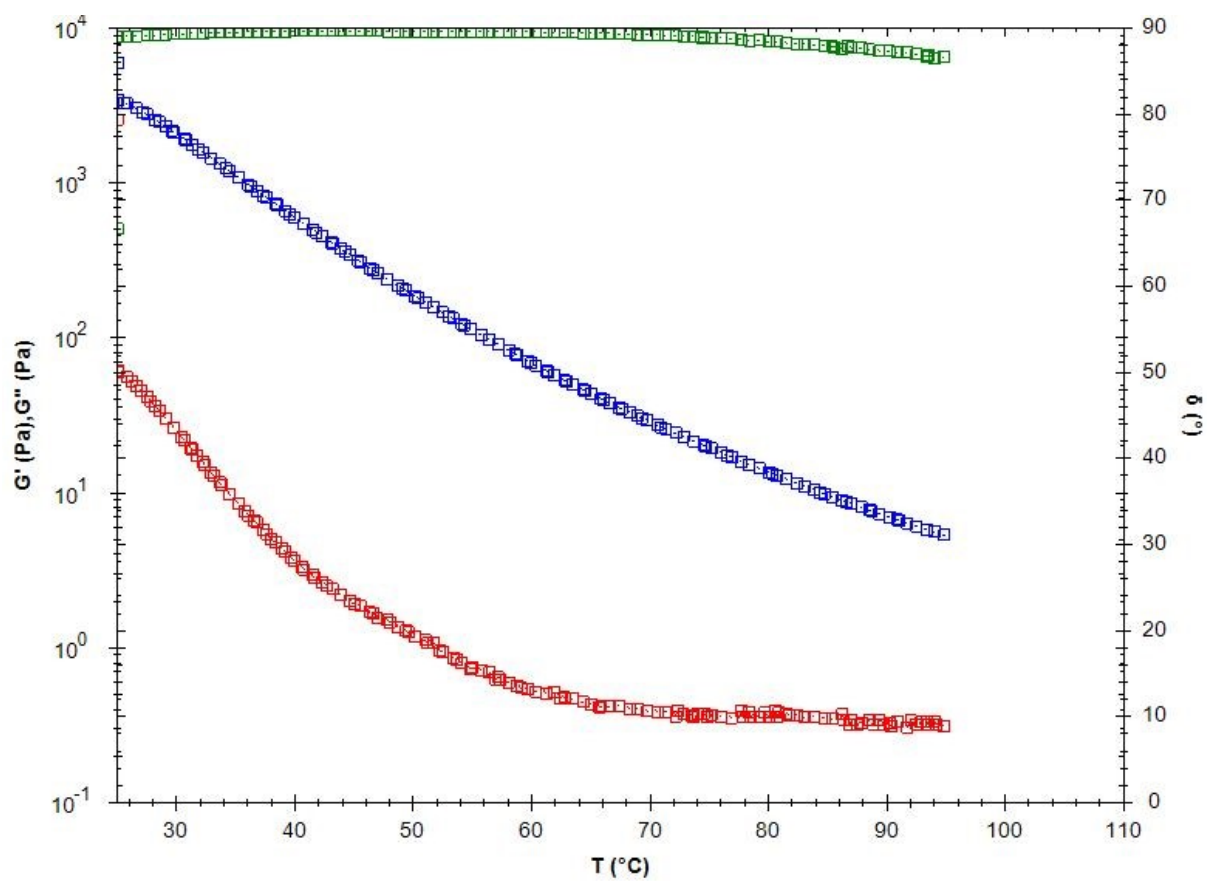


**Figure 23** Temperature dependence of elastic modulus  $G'$  (red), viscous modulus  $G''$  (blue), and phase angle  $\delta$  (green) of 3T plasticized with 30% of TA.

### 3.3. Adhesive properties

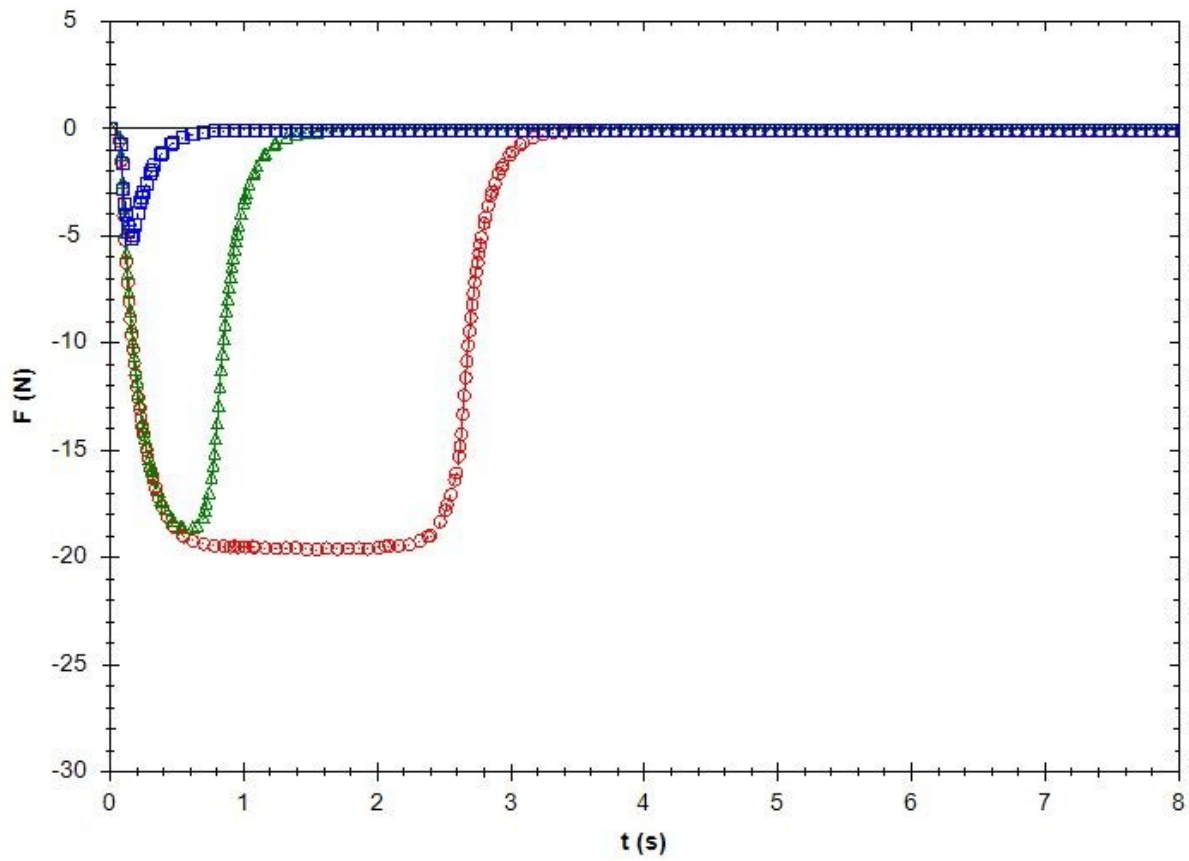


**Figure 24** Adhesive force  $F$  (N) of PLGA: EP (blue), MS (green) and TA (red). Plasticizer concentration 30%, temperature 25 °C

**Table 17** Values of adhesive force for PLGA plasticized with 30% of EP, MS and TA at 25 °C.

Measurement	PLGA + 30% EP F (N)	PLGA + 30% MS F (N)	PLGA + 30% TA F (N)
1.	5.43	18.46	19.67
2.	5.11	18.85	19.64
3.	4.89	18.91	19.68
4.	5.44	18.64	19.64
5.	4.91	18.39	19.66
Average $\pm$ SD	5.16 $\pm$ 0.24	18.65 $\pm$ 0.19	19.66 $\pm$ 0.02

**Table 18** Values of time necessary to decrease the force by 90% for PLGA plasticized with 30% of EP, MS and TA at 25 °C.

Measurement	PLGA + 30% EP t (s)	PLGA + 30% MS t (s)	PLGA + 30% TA t (s)
1.	0.5121	1.030	1.550
2.	0.5133	1.159	2.919
3.	0.5110	1.089	3.060
4.	0.5137	1.003	2.827
5.	0.5142	1.089	3.095
Average $\pm$ SD	0.5129 $\pm$ 0.0012	1.074 $\pm$ 0.054	2.690 $\pm$ 0.578

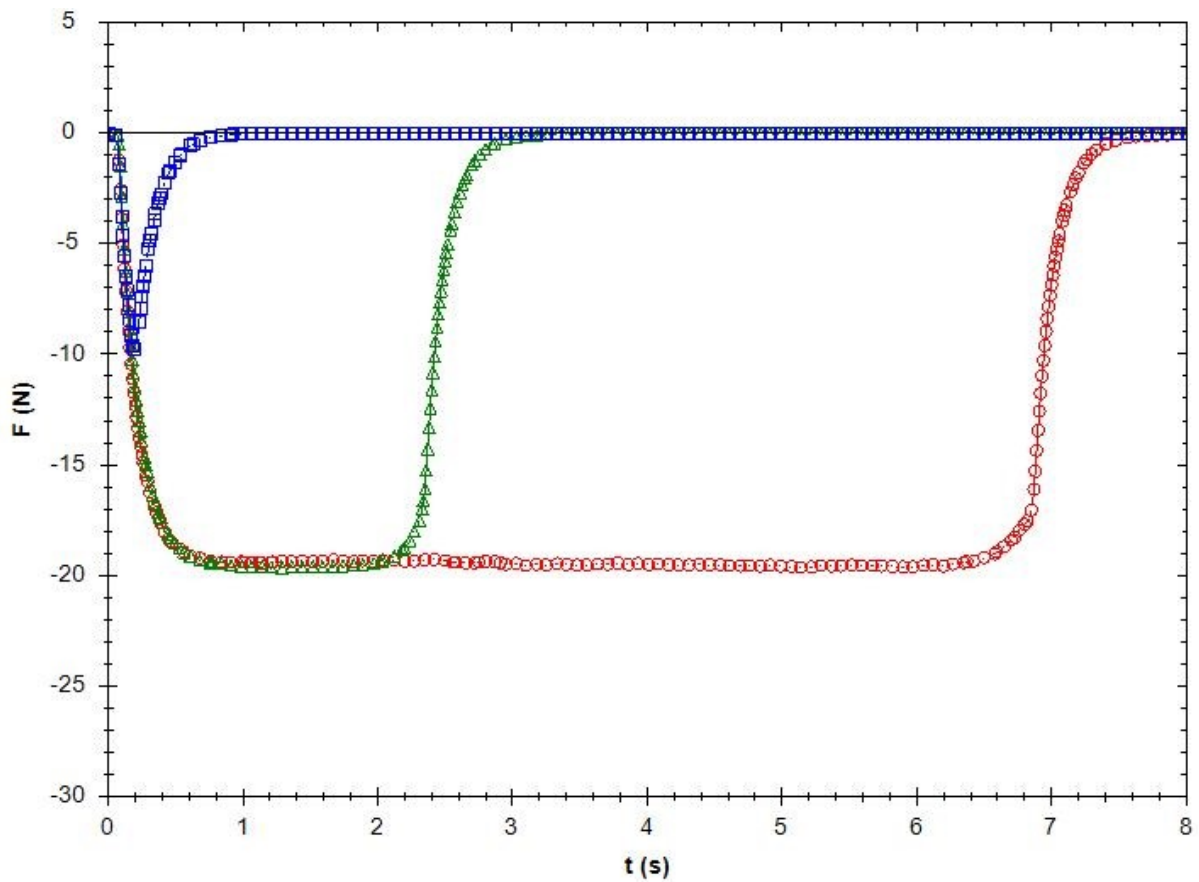


**Figure 25** Adhesive force  $F$  (N) of 2A: EP (blue), MS (green) and TA (red). Plasticizer concentration 30%, temperature 25 °C.

**Table 19** Values of adhesive force for 2A plasticized with 30% of EP, MS and TA at 25 °C.

Measurement	2A + 30 % EP F (N)	2A + 30 % MS F (N)	2A + 30 % TA F (N)
1.	9.72	19.66	19.65
2.	9.38	19.69	19.65
3.	9.31	19.65	19.64
4.	9.75	19.59	19.67
5.	10.15	19.62	19.65
Average $\pm$ SD	9.66 $\pm$ 0.30	19.64 $\pm$ 0.03	19.65 $\pm$ 0.01

**Table 20** Values of time necessary to decrease the force by 90% for 2A plasticized with 30% of EP, MS and TA at 25 °C.

Measurement	2A + 30 % EP t (s)	2A + 30 % MS t (s)	2A + 30 % TA t (s)
1.	0.5680	2.842	7.186
2.	0.5626	2.692	7.747
3.	0.5443	2.655	7.216
4.	0.5368	2.216	7.388
5.	0.5667	2.102	6.916
Average $\pm$ SD	0.5557 $\pm$ 0.0127	2.501 $\pm$ 0.289	7.291 $\pm$ 0.274

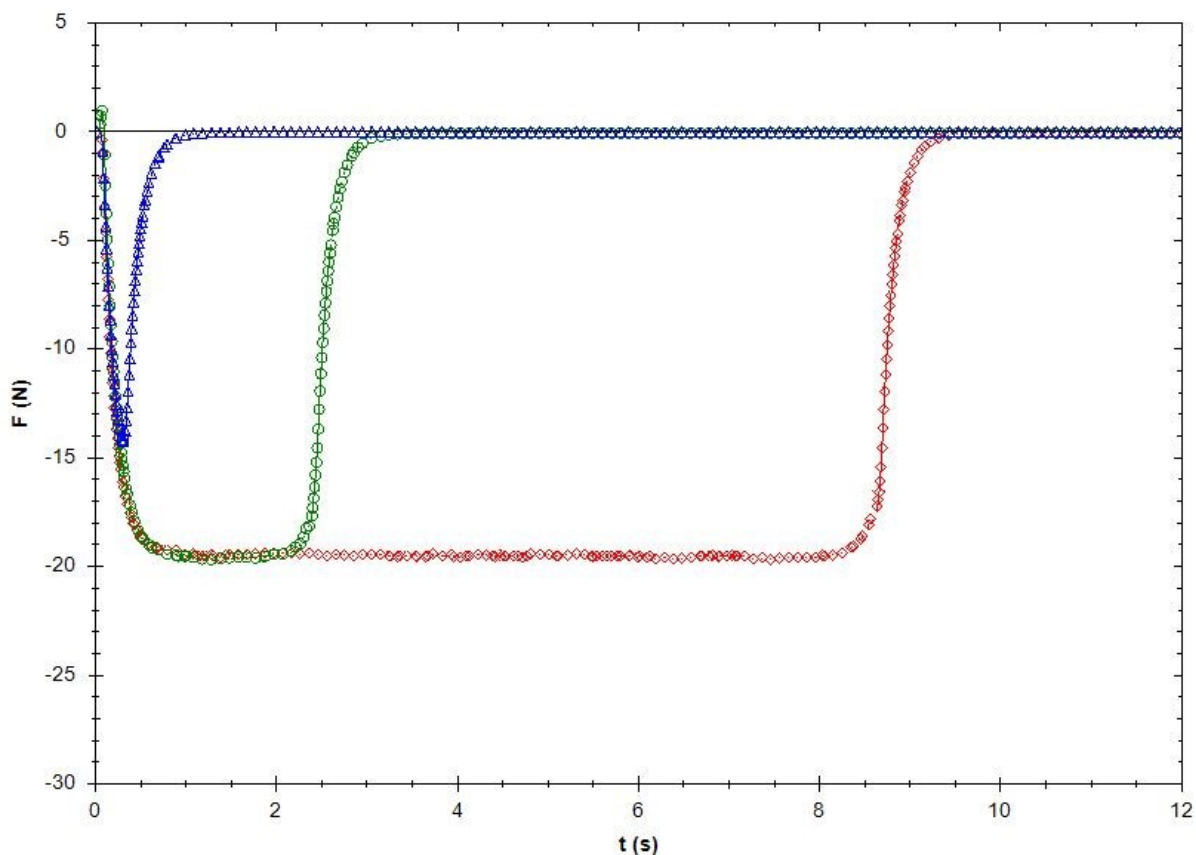


**Figure 26** Adhesive force  $F$  (N) of 3T: EP (blue), MS (green) and TA (red). Plasticizer concentration 30%, temperature 25 °C.

**Table 21** Values of adhesive force for 3T plasticized with 30% of the EP, MS and TA at 25 °C.

Measurement	3T + 30% EP F (N)	3T + 30% MS F (N)	3T + 30% TA F (N)
1.	13.48	19.68	19.67
2.	12.85	19.69	19.66
3.	13.48	19.61	19.67
4.	12.77	19.69	19.63
5.	13.30	19.68	19.63
Average $\pm$ SD	13.18 $\pm$ 0.31	19.67 $\pm$ 0.03	19.65 $\pm$ 0.02

**Table 22** Values of time necessary to decrease the force by 90% for 3T plasticized with 30% of the EP, MS and TA at 25 °C

Measurement	3T + 30% EP t (s)	3T + 30% MS t (s)	3T + 30% TA t (s)
1.	0.6556	2.743	7.217
2.	0.6500	2.762	8.537
3.	0.6360	2.955	8.992
4.	0.6360	2.810	9.925
5.	0.6423	2.965	10.28
Average $\pm$ SD	0.6440 $\pm$ 0.0078	2.847 $\pm$ 0.095	8.99 $\pm$ 1.09

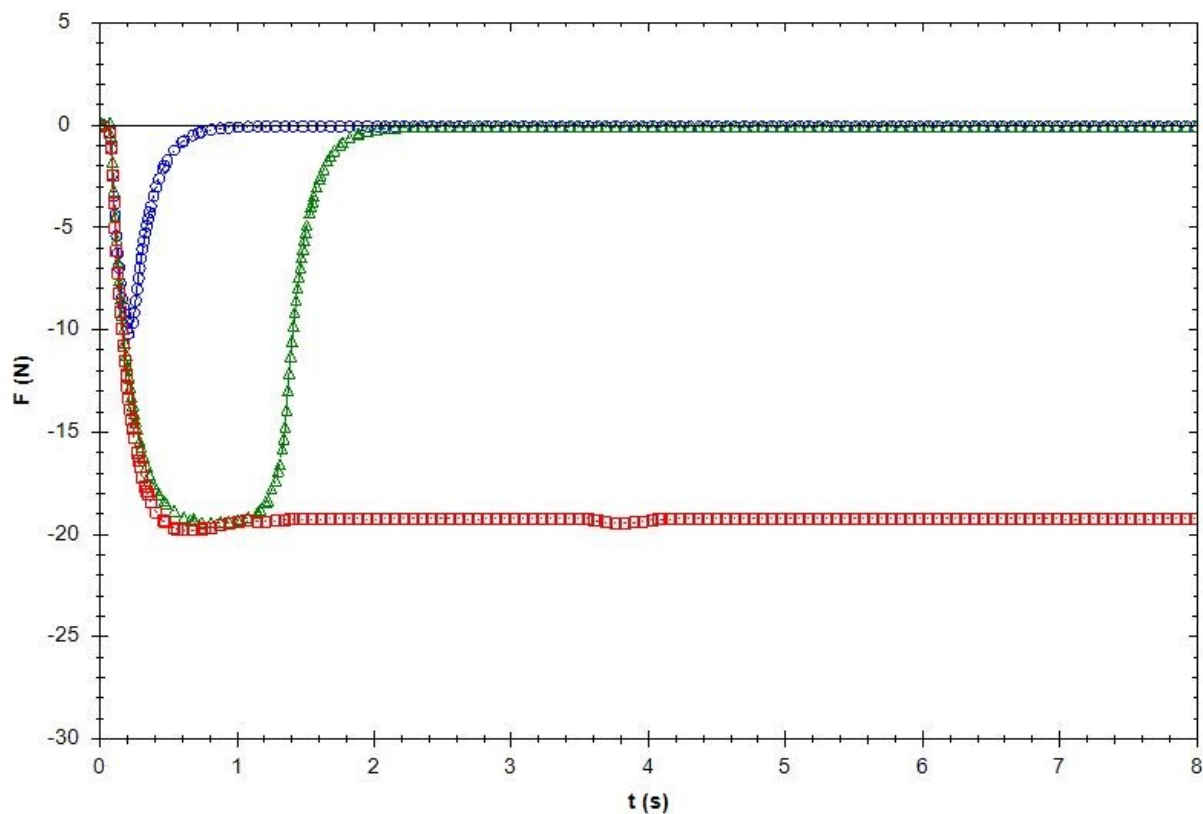


**Figure 27** Adhesive force  $F$  (N) of 8D: 10% (red), 20% (green), and 30% (blue). Plasticizer used methyl salicylate, temperature 25 °C

**Table 23** Values of adhesive force for 8D plasticized with 10, 20 and 30% of MS at 25 °C.

Measurement	8D + 10 % MS F (N)	8D + 20 % MS F (N)	8D + 30 % MS F (N)
1.	19.88	19.40	9.99
2.	19.65	19.50	9.44
3.	20.61	19.49	10.05
4.	19.99	19.43	10.27
5.	19.80	19.48	10.19
Average $\pm$ SD	19.99 $\pm$ 0.33	19.46 $\pm$ 0.04	10.05 $\pm$ 0.31

**Table 24** Values of time necessary to decrease the force by 90% for 8D plasticized with 10, 20 and 30% of MS at 25 °C.

Measurement	8D + 10 % MS t (s)	8D + 20 % MS t (s)	8D + 30 % MS t (s)
1.	43.31	1.558	0.5601
2.	43.87	1.774	0.5451
3.	51.35	1.788	0.5710
4.	53.66	1.644	0.5669
5.	47.94	1.791	0.5687
Average $\pm$ SD	48.03 $\pm$ 4.06	1.711 $\pm$ 0.094	0.5624 $\pm$ 0.0094

### 3.4. SEM

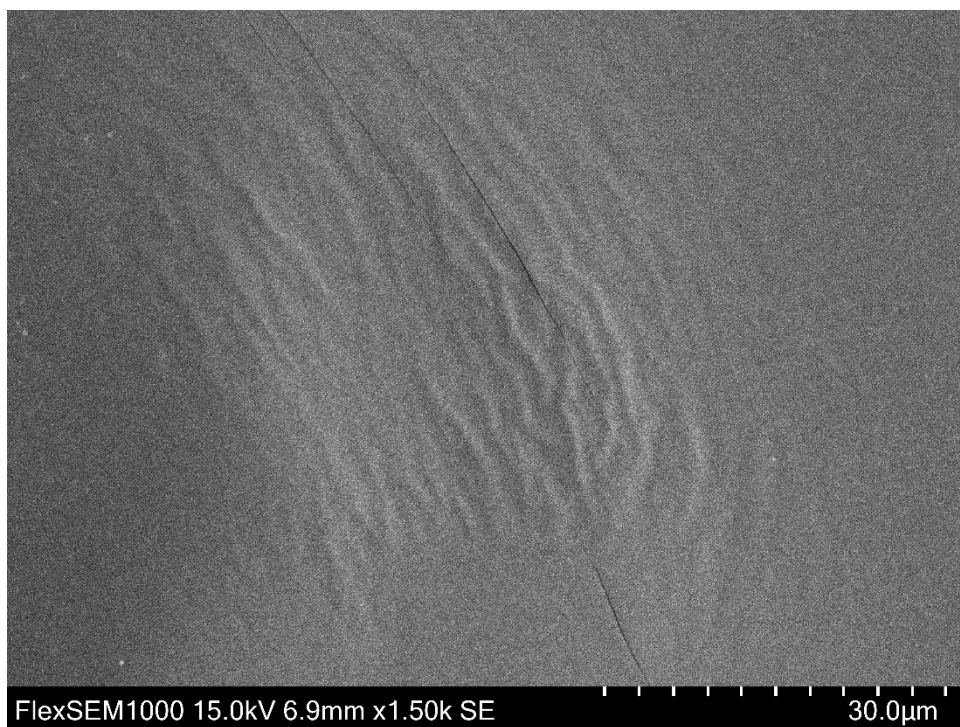


*Figure 28 SEM image of top surface of non-plasticized in situ film (2A, salicylic acid 5%)*

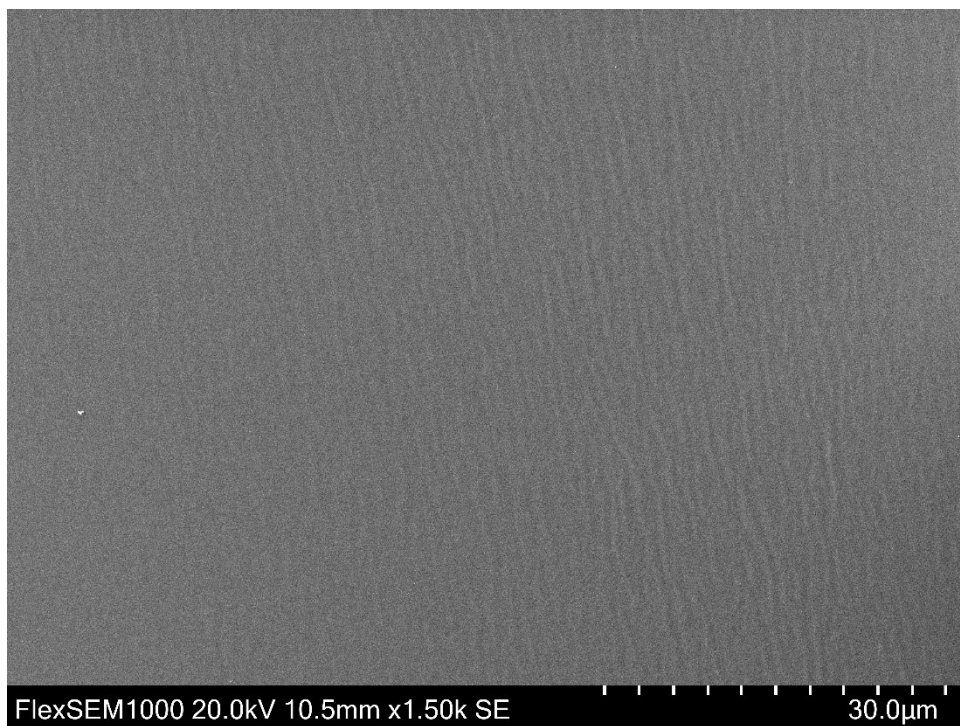


*Figure 29 SEM image of top surface of plasticized in situ film (2A, salicylic acid 5%, methyl salicylate 30%)*



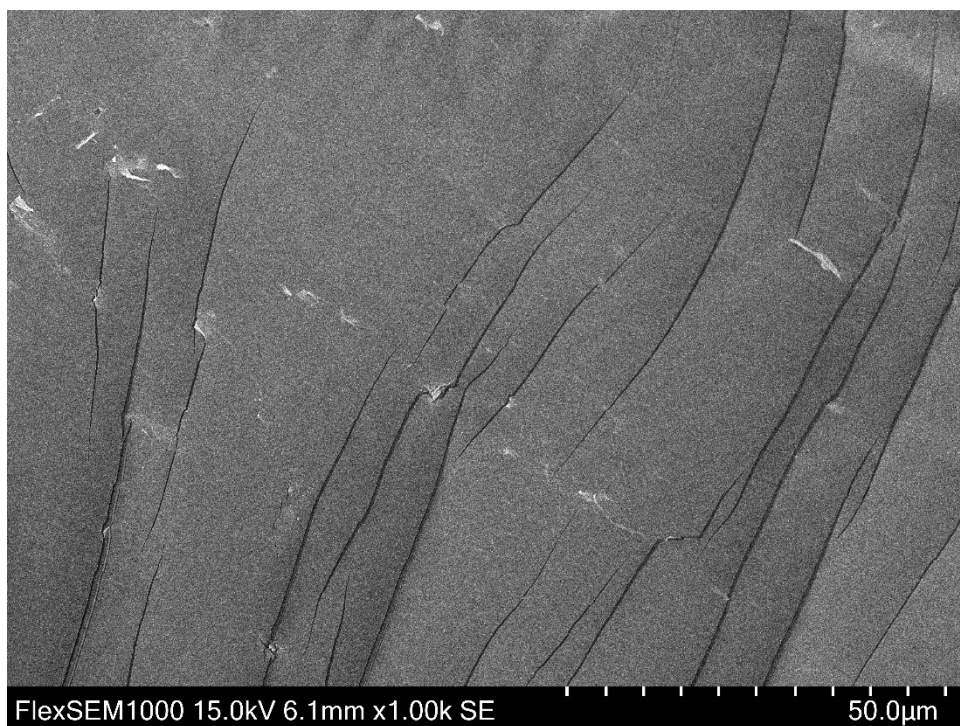


**Figure 30** SEM image of fracture surface of non-plasticized in situ film (2A, salicylic acid 5%)

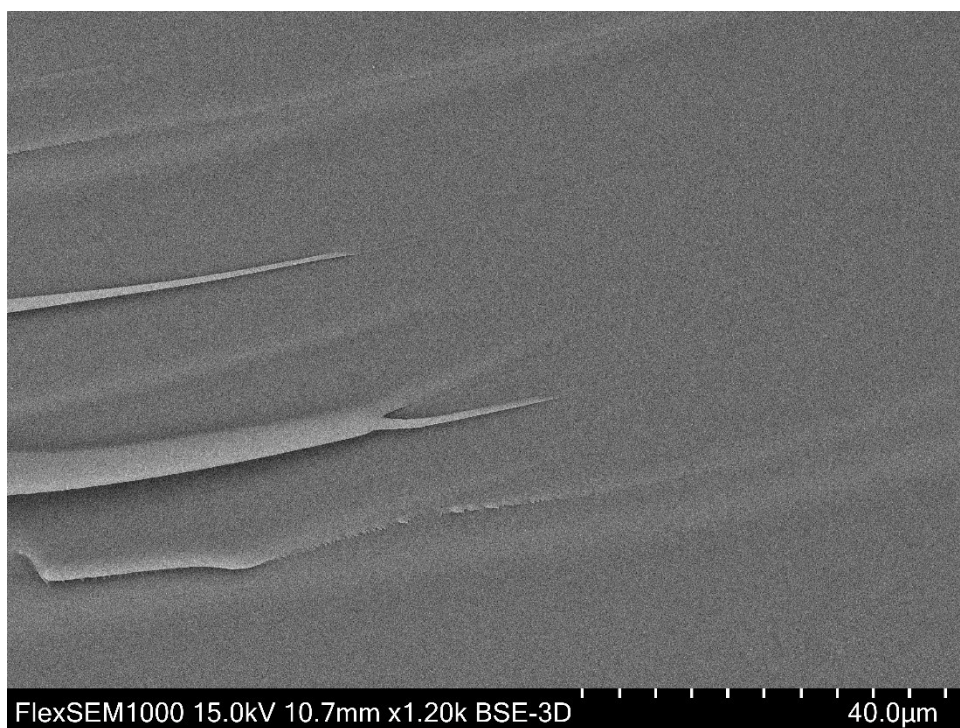


**Figure 31** SEM image of fracture surface of plasticized in situ film (2A, salicylic acid 5%, methyl salicylate 30%)

### 3.5. Drug release

**Table 25** Dissolution of salicylates (SAL) from FFS made of 75% of 2A, 5% of salicylic acid and 20% of methyl salicylate.

Time [h]	Absorbance	Dilution	SAL [mg]	SAL [%]	Average [%]	Cumulative [%]
5	1.3522	10	5.2227	5.85	5.57	5.57
	1.3447	10	5.1933	5.82		
	1.1656	10	4.4910	5.03		
24	1.4726	10	5.6949	6.38	5.81	11.38
	1.5821	10	6.1244	6.86		
	0.9719	10	3.7315	4.18		
48	1.1098	10	4.2720	4.79	5.58	16.96
	1.4567	10	5.6324	6.31		
	1.3027	10	5.0286	5.63		
72	1.3146	10	5.0752	5.69	6.04	23.00
	1.6925	10	6.5571	7.35		
	1.1751	10	4.5282	5.07		
96	1.1840	10	4.5633	5.11	5.24	28.24
	1.4337	10	5.5424	6.21		
	1.0240	10	3.9358	4.41		
144	1.7187	10	6.6601	7.46	6.20	34.44
	1.5596	10	6.0362	6.76		
	1.0175	10	3.9102	4.38		
264	1.3081	16.67	8.4180	9.43	8.31	42.75
	1.2967	16.67	8.3433	9.35		
	0.8585	16.67	5.4791	6.14		

**Table 26** Dissolution of salicylates (SAL) from FFS containing 80% of 2A, 10% of salicylic acid and 10% of methyl salicylate.

Time [h]	Absorbance	Dilution	SAL [mg]	SAL [%]	Average [%]	Cumulative [%]
5	1.2272	16.67	7.8892	10.04	10.16	10.16
	1.2570	16.67	8.0842	10.29		
	1.0590	16.67	6.7898	8.64*		
24	1.0831	16.67	6.9469	8.84	8.82	18.98
	1.0792	16.67	6.9216	8.81		
	0.8135	16.67	5.1847	6.60*		
48	0.7567	16.67	4.8134	6.12	6.80	25.78
	0.9193	16.67	5.8761	7.48		
	0.7022	16.67	4.4573	5.67*		
72	1.4808	10	5.7269	7.29	7.82	33.61
	1.6962	10	6.5718	8.36		
	1.2055	10	4.6473	5.91*		
96	1.5532	10	6.0111	7.65	7.56	41.17
	1.5188	10	5.8761	7.48		
	0.8822	10	3.3795	4.30*		
144	1.7466	16.67	11.2846	14.36	13.63	54.79
	1.5708	16.67	10.1351	12.89		
	0.5826	16.67	3.6750	4.68*		
264	1.6941	16.67	10.9416	13.92	13.48	68.28
	1.5893	16.67	10.2565	13.05		
	1.2330	16.67	7.9271	10.09*		

\* the value was not included in the average

**Table 27** Dissolution of salicylates (SAL) from FFS containing 85% of 2A, 5% of salicylic acid and 10% of methyl salicylate.

Time [h]	Absorbance	Dilution	SAL [mg]	SAL [%]	Average [%]	Cumulative [%]
5	0.9185	10	3.5221	6.58	7.09	7.09
	0.9778	10	3.7545	7.01		
	1.0679	10	4.1077	7.67		
24	1.0727	10	4.1265	7.71	8.69	15.78
	1.1192	10	4.3092	8.05		
	1.4287	10	5.5227	10.31		
48	0.9461	10	3.6303	6.78	7.84	23.61
	0.9456	10	3.6284	6.78		
	1.3809	10	5.3354	9.96		
72	0.8187	10	3.1306	5.85	7.04	30.66
	0.9285	10	3.5610	6.65		
	1.1990	10	4.6218	8.63		
96	0.6062	10	2.2974	4.29	6.65	37.30
	1.0404	10	3.9999	7.47		
	1.1380	10	4.3827	8.18		
144	0.7002	10	2.6659	4.98	10.02	47.33
	1.6498	10	6.3899	11.93		
	1.8169	10	7.0451	13.16		
264	0.5145	16.67	3.2298	6.03	10.44	57.77
	1.0450	16.67	6.6983	12.51		
	1.0679	16.67	6.8476	12.79		

## 4 DISCUSSION

PLGA as well as derived polyesters branched on polyacrylic acid (2A), tripentaerythritol (3T), and dipentaerythritol (8D) are too viscous and brittle under ambient conditions which limits their practical use in the formulation of thin films. Decrease of viscosity and optimization of elastic properties might be achieved by employing a suitable plasticizer. This might apart from the plasticizing also show other beneficial activities. For this work three different plasticizers with additional advantageous properties were chosen: ethyl pyruvate (EP) and methyl salicylate (MS) with anti-inflammatory activity and triacetin (TA) with proven antifungal activity. Both plasticized and non-plasticized PLGA derivatives were subject of thermal analysis while the rheological and adhesion testing was performed with the plasticized polymers only. Furthermore, salicylic acid loaded FFSs based on 2A and plasticized with methyl salicylate were formulated with subsequent SEM imaging and drug release testing.

### 4.1. DSC

The obtained values of glass transition temperature of non-plasticized polymers confirmed those published by Šnejdrová et al.<sup>38</sup> with exception of 8D (**Table 9**). Considerable drop, from 12.4 to 1.9 °C, in  $T_g$  of this polymer was noted pointing to the time connected degradation of this polymer. Incorporation of salicylic acid itself or in combination with ethyl pyruvate as a plasticizer led to the decrease of  $T_g$ . The largest drop was recorded in 2A with 20% of the salicylic acid and no plasticizer leading to a conclusion that 20% of salicylic acid show better plasticizing properties than its lower concentration in combination with 10% of EP. This correlates with the fact that salicylic acid is structurally close to methyl salicylate which is an efficient plasticizer. Furthermore, at 108.9 °C there is a second peak on the thermic curve of this system which might signify presence of a crystalline phase and its melting.

### 4.2. Rheological testing

Viscosity curves of all tested plasticized polyesters showed minimal changes in viscosity with increasing shear rate (example at **Figure 14**, **Figure 15**, **Figure 16**). Unfortunately, no exact limits are defined for the drop in viscosity which would signify pseudoplastic instead of Newtonian behavior. The correlation to Newton and Power law models was used to determine the change of viscosity with increasing shear rate. The flow curves correlated to both models, (**Table 10**, **Table 11**, **Table 12**) in all measured systems but based on the values of power law index ( $n$ ) approaching value of 1 it can be concluded that the tested plasticized polymers PLGA, 2A and 3T show Newtonian behavior. In case of 8D where dependency of viscosity on

concentration of plasticizer was studied, a slight shift to pseudoplastic behavior was observed under the highest temperature (50 °C) and the highest concentration of plasticizer (30% MS), this is supported by both the course of the viscosity curve (**Figure 19**) as well as the drop in the value of power law index (**Table 13**). Although the values of viscosity for 3T plasticized with the highest concentration (40%) of EP at 37 °C (**Table 14**) were similar to those of 8D plasticized with 30% of MS at 50 °C, the viscosity curve remained in correlation with Newtonian behavior (**Figure 20**).

Obtained viscosity values of PLGA, 2A and 3T plasticized with the same concentration of the same plasticizer revealed that PLGA plasticized with 30% of EP is approximately twice less viscous than 2A and three times less viscous than 3T plasticized with the same concentration of EP. When plasticized with 30% of MS or TA, viscosity values of PLGA were three times lower than those of the both branched polymers plasticized with the same plasticizers at the same concentration (**Table 10, Table 11, Table 12**). The fact that molar weight of linear PLGA ( $M_w = 2400 \text{ g}\cdot\text{mol}^{-1}$ ) is six times lower than the molar weight of branched polymers 2A and 3T leads to the conclusion that viscosity is influenced by the molar weight of the polymer. This effect was not temperature dependent.

Three different substances were tested as plasticizers: ethyl pyruvate, methyl salicylate and triacetin. Use of all led to the expected decrease in viscosity, the most efficient proved to be ethyl pyruvate followed by methyl salicylate and triacetin (**Figure 32**). The same dependency was observed at all tested temperatures.

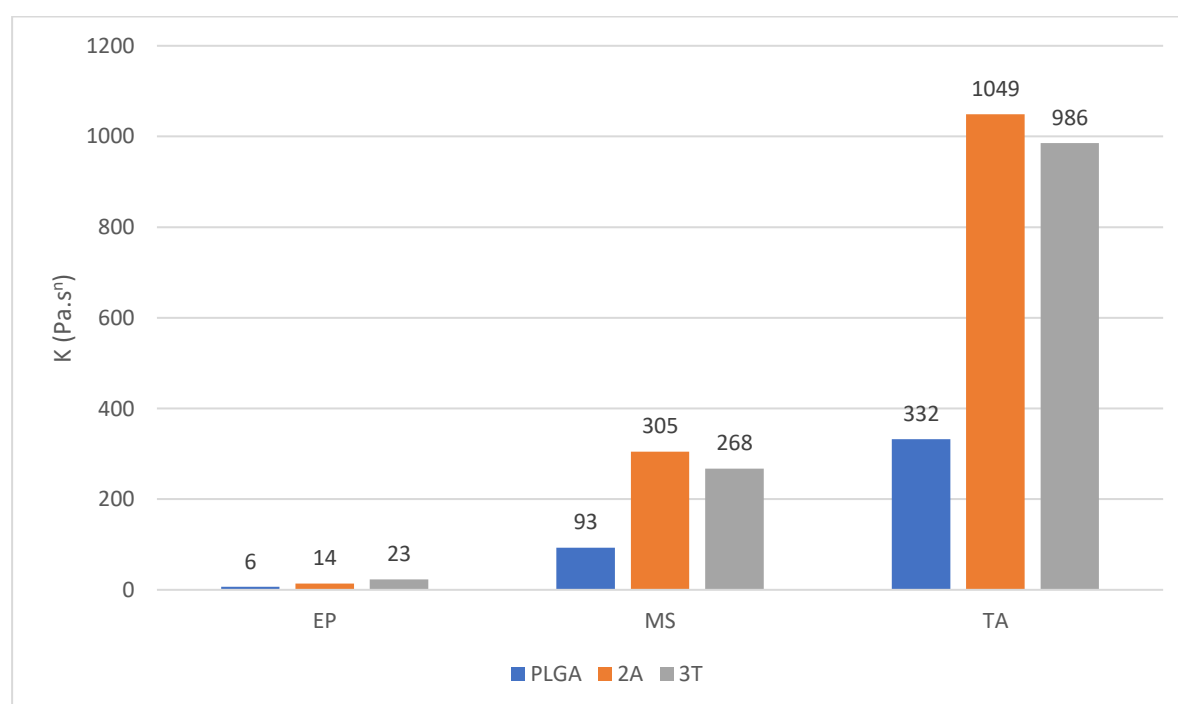


**Figure 32** Effect of different plasticizers in concentration of 30% on consistency index K at 25 °C.

Dependency of viscosity on plasticizer concentration was studied with 8D plasticized with 10, 20 and 30% of methyl salicylate at 25, 37 and 50 °C (**Figure 17**, **Figure 18**, **Figure 19**) and 3T plasticized with 10, 20, 30 and 40% of ethyl pyruvate at 37 °C (**Figure 20**). It was confirmed that the viscosity drops with the increasing concentration of plasticizer. Same as for the other polymers the efficiency of plasticizer decreased with the increasing temperature.

The temperatures were chosen based on the conditions typical for topical application (25 °C), physiological temperature of human body (37 °C) and maximum temperature for application to the human body (50 °C). Due to the fact that viscosity is a temperature dependent parameter drop of its values with growing temperature was expected and confirmed. The clearly observable difference in viscosity values of PLGA plasticized with the same concentration of different plasticizers at 25 °C was minimal at 50 °C (**Figure 33**) showing that the temperature influence on viscosity is greater than the effect of plasticizer. The same was observed by 2A and 3T as well.

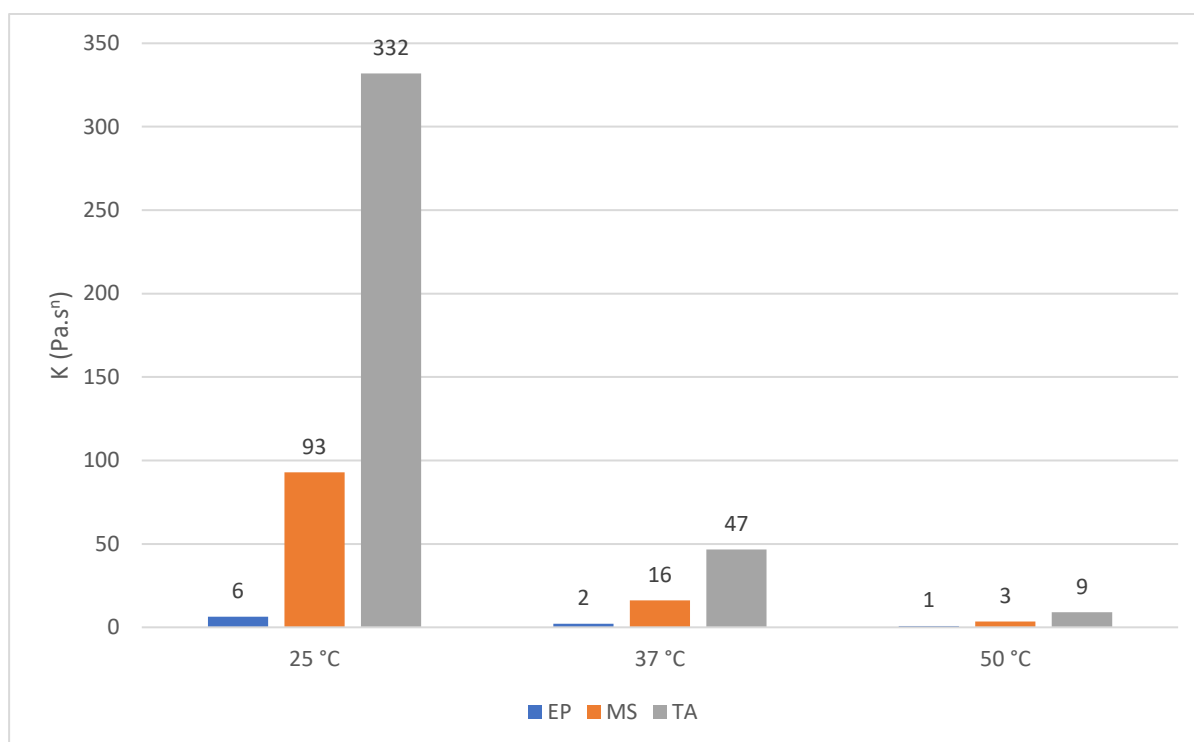


**Figure 33** Effect of different temperature on consistency index  $K$  of polymer PLGA plasticized with 30 % of EP, MS or TA.

The values of viscous modulus exceeding those of elastic modulus obtained from oscillation testing and phase angle close to  $90^\circ$  revealed that the plasticized polymers 8D and 3T are viscoelastic liquids without an inner structure typical for solid systems at  $25^\circ\text{C}$  in the range of strain from 0.01 to 100% (**Table 15**, **Table 16**). Although the values of viscous resp. elastic modulus decreased with increasing concentration of plasticizer by 8D, their ratio remained greater than 1 and didn't reach the point of gelation where  $G'' = G'$ . Moreover, the phase angle remained at  $90^\circ$  confirming liquid-like nature of the system (**Figure 21**). For 3T temperature dependency of the moduli and phase angle was measured in range of 25 to  $95^\circ\text{C}$  (**Figure 23**) and showed decrease of both moduli with temperature growth. Most importantly, the ratio of viscous to elastic modulus also decreased at higher temperatures and from  $62^\circ\text{C}$  slight reduction of phase angle was observed indicating possible creation of rigid structures.

### 4.3. Adhesion

The adhesive forces expressed as force necessary to separate the plates showed correlation with viscosity - the lower the viscosity the lower the adhesion. Thus, the lowest adhesion was observed by the polymers plasticized with ethyl pyruvate (**Figure 34**). Although the values of force necessary to separate the plates were often similar for the individual polymer plasticized with MS and TA, the difference in adhesion was given by the longer time necessary to decrease the force by 90% (**Figure 24**, **Figure 25**, **Figure 26**). This time was on average 3 times longer by the polymers plasticized with TA then by those plasticized with MS (**Table 18**, **Table 20**, **Table 22**). By 8D plasticized with MS the adhesion dropped with increasing concentration of the plasticizer (**Figure 27**) which is in accordance with the previously mentioned decrease in adhesion with lower viscosity. The adhesive force of the sample plasticized with only 10% of MS was much greater than by the higher concentrations of MS so it was not possible to plot its drop into the chart within the visible range of time.



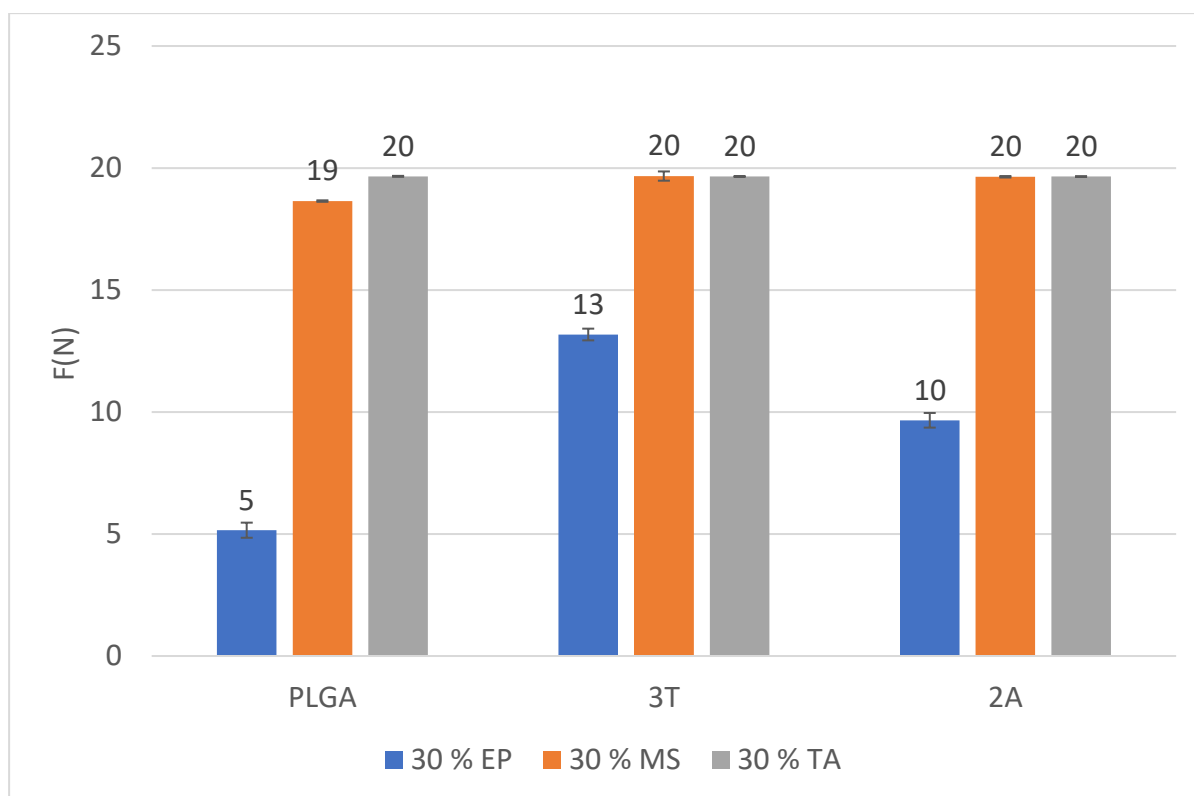


**Figure 34** Effect of different plasticizers on adhesion of polymers PLGA, 2A and 3T

#### 4.4. SEM

The SEM observations of films composed of 2A and 5% of salicylic acid without plasticizer or with 30% of MS were performed and the resulting images are shown in **Figure 28**, **Figure 29**, **Figure 30** and **Figure 31**. Both films are homogeneous on their top surface as well as inside the material indicating complete dissolution of the drug. However, the top surface of the non-plasticized 2A film shows small longitudinal cracks (**Figure 28**) that might have been caused by shear stress applied during the preparation of the sample for the SEM measurement. The top surface of plasticized 2A film is almost perfectly smooth without pores and structural defects (**Figure 29**). The same is true for its fracture surface while the fracture surface of the non-plasticized variant shows several cracks indicating its higher fragility (**Figure 30**). Based on these findings, it can be concluded that polymer 2A with suitable plasticizer can form a firm, homogenous, non-porous film which shows certain degree of elasticity important for skin application.

#### 4.5. Drug release

FFSs for trial drug release tests were prepared with polymer 2A, salicylic acid and methyl salicylate. Salicylic acid was chosen as a model drug for drug release testing due to its good availability and fact, that it's often used for topical delivery of salicylates. Methyl salicylate

was the plasticizer of choice because it is also a prodrug of salicylates and increases the amount of delivered salicylates<sup>36</sup>. Salicylic acid was incorporated in concentration of 5% or 10%, methyl salicylate in concentration of 10% or 20%. In the period of 11 days 43% of the salicylates was detected to be released from the formulation with 20% of methyl salicylate, whereas in the FFSs with lower concentration of methyl salicylate (10%) 68% resp. 58% of salicylates was found to be released (**Figure 35**). As there were no film residues present after 11 days the expectation is that all salicylates were released proving the spectrophotometric method not suitable for their quantitative determination. Based on the obtained results it can be stated that liberation is reduced with higher concentration of methyl salicylate. Furthermore, the use of 2A lead to the prolonged release of salicylic acid which is advantageous for single-dose treatment. No release lag-time as well as initial burst was observed at any FFS. Dissolution profiles displayed linear dependence on the time between 5 and 96 hours which is in compliance with the findings made by Andreopoulos et al. in 2001 with poly(D,L-Lactide)<sup>74</sup> (**Figure 36**). However, further research is necessary to confirm this. To assess the concentration of released salicylates more accurately, HPLC method is recommended for future testing.

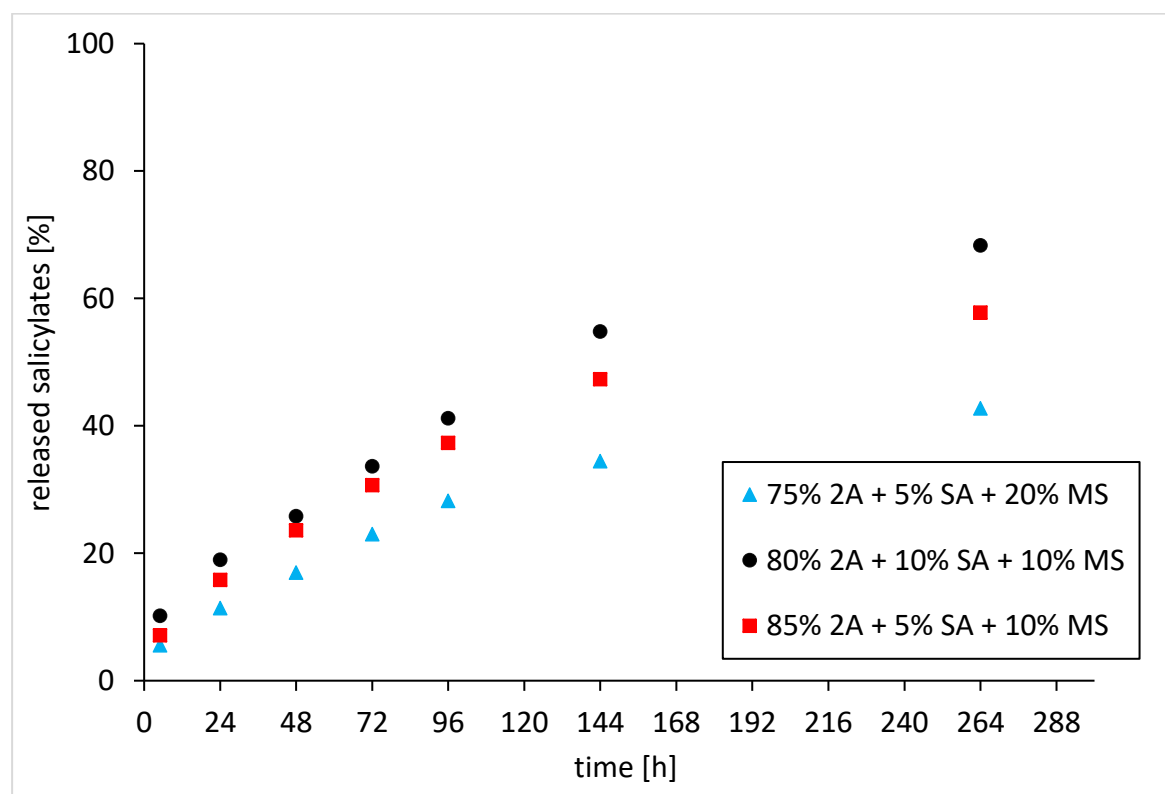


**Figure 35** Dissolution profiles of FFS containing 2A, salicylic acid and methyl salicylate in different ratios.

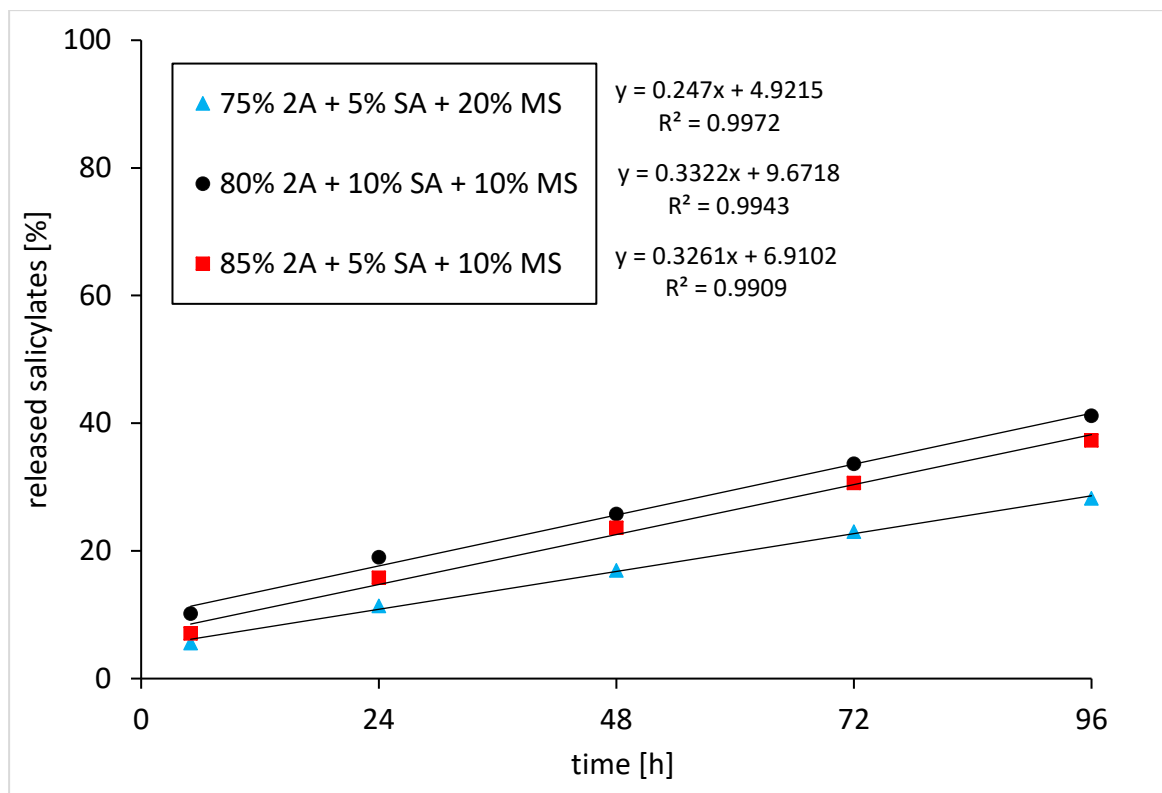


**Figure 36** Linear course of dissolution profiles of FFS containing 2A, salicylic acid and methyl salicylate in different ratios in time range from 5 h to 96 h.

## 5 CONCLUSIONS

When combined with suitable plasticizer, PLGA as well as its derivatives branched on tripentaerythritol (3T), polyacrylic acid (2A) or dipentaerythritol (8D) have adequate thermal, rheological and adhesive properties for use in film forming systems (FFSs). After plasticization all tested polymers showed Newtonian behavior with shear rate independent viscosity. From the three tested plasticizers, ethyl pyruvate was the most efficient one leading to the largest drop in viscosity. However, for formulation of salicylic acid loaded FFSs methyl salicylate was preferred over ethyl pyruvate because besides having plasticizing properties it is also a source of salicylates. Combination of 2A and methyl salicylate enabled successful formulation of salicylic acid FFSs. SEM imaging confirmed the homogenous state of the film and effect of the plasticizer on its mechanical properties. Release of salicylates showed linear pattern within the first four days.

## **6 ACNOWLEDGEMENTS**

Hereby I would like to thank to Mgr. Jan Loskot, Ph.D. for performing the SEM testing and to Doc. RNDr. Milan Dittrich, Ph.D. for synthesis of all polymers used in the experimental part. Special thank goes to Mgr. Juraj Martiška, Ph.D. for valuable advices in rheological testing and technical support.

## 7 REFERENCES

1. Kathe K, Kathpalia H. Film forming systems for topical and transdermal drug delivery. *Asian J Pharm Sci.* 2017;12(6):487-497. doi:10.1016/j.ajps.2017.07.004
2. Misra A, Raghuvanshi RS, Ganga S, Diwan M, Talwar GP, Singh O. Formulation of a transdermal system for biphasic delivery of testosterone. *J Control Release.* 1996;39(1):1-7. doi:10.1016/0168-3659(95)00122-0
3. Zurdo Schroeder I, Franke P, Schaefer UF, Lehr C-M. Development and characterization of film forming polymeric solutions for skin drug delivery. *Eur J Pharm Biopharm.* 2007;65(1):111-121. doi:10.1016/j.ejpb.2006.07.015
4. Tran TTD, Tran PHL. Controlled release film forming systems in drug delivery: The potential for efficient drug delivery. *Pharmaceutics.* 2019;11(6):1-16. doi:10.3390/pharmaceutics11060290
5. Tan X, Feldman SR, Chang J, Balkrishnan R. Topical drug delivery systems in dermatology: a review of patient adherence issues. *Expert Opin Drug Deliv.* 2012;9(10):1263-1271. doi:10.1517/17425247.2012.711756
6. McAuley WJ, Caserta F. Film-Forming and Heated Systems. In: *Novel Delivery Systems for Transdermal and Intradermal Drug Delivery.* John Wiley & Sons, Ltd; 2015:97-124. doi:10.1002/9781118734506.ch5
7. Frederiksen K, Guy RH, Petersson K. Formulation considerations in the design of topical, polymeric film-forming systems for sustained drug delivery to the skin. *Eur J Pharm Biopharm.* 2015;91:9-15. doi:10.1016/j.ejpb.2015.01.002
8. GlaxoSmithKline Group of Companies. Lamisil. Accessed October 29, 2020. <https://www.lamisil-info.de/lamisil-mittel-gegen-hautpilz/lamisil-once/>
9. ZARS I. *Pliaglis (Lidocaine and Tetracaine) Cream 7% / 7%.*; 2007. [https://www.accessdata.fda.gov/drugsatfda\\_docs/label/2007/021717s002lbl.pdf](https://www.accessdata.fda.gov/drugsatfda_docs/label/2007/021717s002lbl.pdf)
10. Perrigo Pharma International D.A.C. Evamist. Accessed October 29, 2020. <https://www.evamist.com/about-evamist/>
11. Acrux Limited. Acrux. Accessed October 29, 2020. <https://www.acrux.com.au/what-we-do/research-development/product-pipeline/>
12. Frederiksen K, Guy RH, Petersson K. The potential of polymeric film-forming systems as sustained delivery platforms for topical drugs. *Expert Opin Drug Deliv.* 2016;13(3):349-360. doi:10.1517/17425247.2016.1124412

13. Felton LA. Mechanisms of polymeric film formation. *Int J Pharm.* 2013;457(2):423-427. doi:10.1016/j.ijpharm.2012.12.027
14. Bos JD, Meinardi MMHM. The 500 Dalton rule for the skin penetration of chemical compounds and drugs. *Exp Dermatol.* 2000;9(3):165-169. doi:10.1034/j.1600-0625.2000.009003165.x
15. Brown MB, Martin GP, Jones SA, Akomeah FK. Dermal and Transdermal Drug Delivery Systems: Current and Future Prospects. *Drug Deliv.* 2006;13(3):175-187. doi:10.1080/10717540500455975
16. Thomas BJ, Finnin BC. The transdermal revolution. *Drug Discov Today.* 2004;9(16):697-703. doi:10.1016/S1359-6446(04)03180-0
17. Schröder IZ. Film forming polymeric solutions as drug delivery systems for the skin [PhD thesis]. Published online 2007.
18. Khasraghi AH, Thomas LM. Preparation and evaluation of lornoxicam film-forming gel. *Drug Invent Today.* 2019;11(8):1906-1913.
19. Gennari CGM, Selmin F, Minghetti P, Cilurzo F. Medicated Foams and Film Forming Dosage Forms as Tools to Improve the Thermodynamic Activity of Drugs to be Administered Through the Skin. *Curr Drug Deliv.* 2019;16(5):461-471. doi:10.2174/1567201816666190118124439
20. Labella Lorite M, Gonzalez J, Fernandez FC. In situ bioadhesive film-forming system for topical delivery of mometasone furoate: Characterization and biopharmaceutical properties. *J Drug Deliv Sci Technol.* 2020;59(May):101852. doi:10.1016/j.jddst.2020.101852
21. Šveikauskaite I, Briedis V. Effect of film-forming polymers on release of naftifine hydrochloride from nail lacquers. *Int J Polym Sci.* 2017;2017. doi:10.1155/2017/1476270
22. Gohel MC, Nagori SA. Fabrication of modified transport fluconazole transdermal spray containing ethyl cellulose and eudragit® RS100 as film formers. *AAPS PharmSciTech.* 2009;10(2):684-691. doi:10.1208/s12249-009-9256-8
23. Lunter DJ, Daniels R. New film forming emulsions containing Eudragit® NE and/or RS 30D for sustained dermal delivery of nonivamide. *Eur J Pharm Biopharm.* 2012;82(2):291-298. doi:10.1016/j.ejpb.2012.06.010
24. Kim Y, Beck-Broichsitter M, Banga AK. Design and evaluation of a poly(Lactide-co-glycolide)-based in situ film-forming system for topical delivery of trolamine salicylate. *Pharmaceutics.* 2019;11(8). doi:10.3390/pharmaceutics11080409

25. Huanbutta K, Sittikijyothin W, Sangnim T. Development of topical natural based film forming system loaded propolis from stingless bees for wound healing application. *J Pharm Investig.* 2020;(0123456789). doi:10.1007/s40005-020-00493-w
26. Jadhav NR, Gaikwad VL, Nair KJ, Kadam HM. Glass transition temperature: Basics and application in pharmaceutical sector. *Asian J Pharm.* 2009;3(2):82-89. doi:10.4103/0973-8398.55043
27. Lecomte F, Siepmann J, Walther M, MacRae RJ, Bodmeier R. Polymer blends used for the aqueous coating of solid dosage forms: importance of the type of plasticizer. *J Control Release.* 2004;99(1):1-13. doi:10.1016/j.jconrel.2004.05.011
28. Lin S-Y, Chen K-S, Run-Chu L. Organic esters of plasticizers affecting the water absorption, adhesive property, glass transition temperature and plasticizer permanence of Eudragit acrylic films. *J Control Release.* 2000;68(3):343-350. doi:10.1016/S0168-3659(00)00259-5
29. Yang F, Yu X, Shao W, et al. Co-delivery of terbinafine hydrochloride and urea with an in situ film-forming system for nail targeting treatment. *Int J Pharm.* 2020;585(May):119497. doi:10.1016/j.ijpharm.2020.119497
30. DrugBank. Salicylic acid. Published 2020. Accessed December 13, 2020. <https://go.drugbank.com/drugs/DB00936>
31. VANE JR. Inhibition of Prostaglandin Synthesis as a Mechanism of Action for Aspirin-like Drugs. *Nat New Biol.* 1971;231(25):232-235. doi:10.1038/newbio231232a0
32. Jacobi A, Mayer A, Augustin M. Keratolytics and Emollients and Their Role in the Therapy of Psoriasis: a Systematic Review. *Dermatol Ther (Heidelb).* 2015;5(1):1-18. doi:10.1007/s13555-015-0068-3
33. Gloor M, Beier B. [Keratoplastic effect of salicylic acid, sulfur and a tensio-active mixture]. *Z Hautkr.* 1984;59(24):1657-1660. <http://www.ncbi.nlm.nih.gov/pubmed/6528692>
34. Kede MPV, Guedes LS. Salicylic Acid Peel. In ; 2017:1-6. doi:10.1007/978-3-319-20252-5\_3-1
35. Randjelović P, Veljković S, Stojiljković N, et al. The Beneficial Biological Properties of Salicylic Acid. *Acta Fac Medicae Naissensis.* 2015;32(4):259-265. doi:10.1515/afmnai-2015-0026
36. Morra P, Bartle WR, Walker SE, Lee SN, Bowles SK, Reeves RA. Serum Concentrations of Salicylic Acid following Topically Applied Salicylate Derivatives. *Ann Pharmacother.* 1996;30(9):935-940. doi:10.1177/106002809603000903



37. Jain RA. The manufacturing techniques of various drug loaded biodegradable poly(lactide-co-glycolide) (PLGA) devices. *Biomaterials*. 2000;21(23):2475-2490. doi:10.1016/S0142-9612(00)00115-0
38. Snejdrova E, Podzimek S, Martiska J, Holas O, Dittrich M. Branched PLGA derivatives with tailored drug delivery properties. *Acta Pharm*. 2020;70(1):63-75. doi:10.2478/acph-2020-0011
39. National Center for Biotechnology Information. PubChem Compound Summary for CID 5541, Triacetin. Accessed November 3, 2020. <https://pubchem.ncbi.nlm.nih.gov/compound/Triacetin>
40. Cosmetic Ingredient Review Expert Panel. Final Report on the Safety Assessment of Triacetin. *Int J Toxicol*. 2003;22(2\_suppl):1-10. doi:10.1080/10915810390204845
41. World Health Organization. Evaluations of the Joint FAO/WHO Expert Committee on Food Additives (JECFA) - Triacetin. Published 2002. Accessed November 6, 2020. <https://apps.who.int/food-additives-contaminants-jecfa-database/chemical.aspx?chemID=3893#>
42. Remington JP. *Remington's Pharmaceutical Sciences*. 18th ed. (Gennaro AR, ed.). Mack Publishing Co.; 1990.
43. National Center for Biotechnology Information. PubChem Compound Summary for CID 12041, Ethyl pyruvate. Published 2020. Accessed November 6, 2020. <https://pubchem.ncbi.nlm.nih.gov/compound/Ethyl-pyruvate>
44. United States Environmental Protection Agency. Propanoic acid, 2-oxo-, ethyl ester 617-35-6 | DTXSID2060674. Published 2015. Accessed November 6, 2020. <https://comptox.epa.gov/dashboard/dsstoxdb/results?search=DTXSID2060674#exposure>
45. Yang R, Han X, Delude RL, Fink MP. Ethyl pyruvate ameliorates acute alcohol-induced liver injury and inflammation in mice. *J Lab Clin Med*. 2003;142(5):322-331. doi:10.1016/S0022-2143(03)00138-0
46. Ulloa L, Ochani M, Yang H, et al. Ethyl pyruvate prevents lethality in mice with established lethal sepsis and systemic inflammation. *Proc Natl Acad Sci*. 2002;99(19):12351-12356. doi:10.1073/pnas.192222999
47. Venkataraman R, Kellum JA, Song M, Fink MP. Resuscitation with Ringer's Ethyl Pyruvate Solution Prolongs Survival and Modulates Plasma Cytokine and Nitrite/Nitrate Concentrations in a Rat Model of Lipopolysaccharide-Induced Shock. *Shock*. 2002;18(6):507-512. doi:10.1097/00024382-200212000-00004

48. Johansson A-S, Johansson-Haque K, Okret S, Palmblad J. Ethyl pyruvate modulates acute inflammatory reactions in human endothelial cells in relation to the NF- $\kappa$ B pathway. *Br J Pharmacol*. 2008;154(6):1318-1326. doi:10.1038/bjp.2008.201
49. Song M, Kellum JA, Kaldas H, Fink MP. Evidence That Glutathione Depletion Is a Mechanism Responsible for the Anti-Inflammatory Effects of Ethyl Pyruvate in Cultured Lipopolysaccharide-Stimulated RAW 264.7 Cells. *J Pharmacol Exp Ther*. 2004;308(1):307-316. doi:10.1124/jpet.103.056622
50. National Center for Biotechnology Information. PubChem Compound Summary for CID 4133, Methyl salicylate. Accessed November 11, 2020. <https://pubchem.ncbi.nlm.nih.gov/compound/Methyl-salicylate#section=Names-and-Identifiers>
51. Norwegian Food Safety Authority. Risk profile Methyl salicylate. 2012;(119):19. [https://www.mattilsynet.no/kosmetikk/stoffer\\_i\\_kosmetikk/risk\\_profile\\_methyl\\_salicylate.9877/binary/Risk Profile Methyl Salicylate](https://www.mattilsynet.no/kosmetikk/stoffer_i_kosmetikk/risk_profile_methyl_salicylate.9877/binary/Risk_Profile_Methyl_Salicylate)
52. DrugBank. Methyl salicylate. Published 2020. Accessed November 11, 2020. <https://go.drugbank.com/drugs/DB09543>
53. EDQM, European Pharmacopoeia C of E. *European Pharmacopoeia*. 10th ed.; 2019.
54. Murdan S, Kerai L, Hossin B. To what extent do in vitro tests correctly predict the in vivo residence of nail lacquers on the nail plate? *J Drug Deliv Sci Technol*. 2015;25:23-28. doi:10.1016/j.jddst.2014.11.002
55. Ghasemlou M, Aliheidari N, Fahmi R, et al. Physical, mechanical and barrier properties of corn starch films incorporated with plant essential oils. *Carbohydr Polym*. 2013;98(1):1117-1126. doi:10.1016/j.carbpol.2013.07.026
56. Wu Y, Qin Y, Yuan M, et al. Characterization of an antimicrobial poly(lactic acid) film prepared with poly( $\epsilon$ -caprolactone) and thymol for active packaging. *Polym Adv Technol*. 2014;25(9):948-954. doi:10.1002/pat.3332
57. Aggarwal R, Targhotra M, Sahoo PK, Chauhan MK. Efinaconazole nail lacquer for the transungual drug delivery: Formulation, optimization, characterization and in vitro evaluation. *J Drug Deliv Sci Technol*. 2020;60(June):101998. doi:10.1016/j.jddst.2020.101998
58. Garvie-Cook H, Frederiksen K, Petersson K, Guy RH, Gordeev S. Characterization of Topical Film-Forming Systems Using Atomic Force Microscopy and Raman Microspectroscopy. *Mol Pharm*. 2015;12(3):751-757. doi:10.1021/mp500582j

59. Tsai M-J, Fu Y-S, Lin Y-H, Huang Y-B, Wu P-C. The Effect of Nanoemulsion as a Carrier of Hydrophilic Compound for Transdermal Delivery. Bansal V, ed. *PLoS One*. 2014;9(7):e102850. doi:10.1371/journal.pone.0102850
60. J Mastropietro D. Rheology in Pharmaceutical Formulations-A Perspective. *J Dev Drugs*. 2013;02(02):2-7. doi:10.4172/2329-6631.1000108
61. Anton Paar GmbH. Basics of rheology. Accessed November 11, 2020. [https://wiki.anton-paar.com/en/basics-of-rheology/?fbclid=IwAR3p1HNGbAGgxh9caf929E4y703OLtSwBGMwAlleauXeA\\_TGqR9xy8b0kcc#rheology-and-rheometryrelated-information](https://wiki.anton-paar.com/en/basics-of-rheology/?fbclid=IwAR3p1HNGbAGgxh9caf929E4y703OLtSwBGMwAlleauXeA_TGqR9xy8b0kcc#rheology-and-rheometryrelated-information)
62. Malvern. *Assessing Tackiness and Adhesion Using a Pull Away Test on a Rotational Rheometer.*; 2015. <https://cdn.technologynetworks.com/TN/Resources/PDF/AN150527AssessingTackinessPullAway.pdf>
63. Minghetti P, Cilurzo F, Casiraghi A. Measuring Adhesive Performance in Transdermal Delivery Systems. *Am J Drug Deliv*. 2004;2(3):193-206. doi:10.2165/00137696-200402030-00004
64. Joshi M, Sharma V, Pathak K. Matrix based system of isotretinoin as nail lacquer to enhance transungual delivery across human nail plate. *Int J Pharm*. 2015;478(1):268-277. doi:10.1016/j.ijpharm.2014.11.050
65. Herrmann S, Daniels R, Lunter D. Methods for the determination of the substantivity of topical formulations. *Pharm Dev Technol*. 2017;22(4):487-491. doi:10.3109/10837450.2015.1135346
66. Ślęzak M. Mathematical models for calculating the value of dynamic viscosity of a liquid. *Arch Metall Mater*. 2015;60(2A):581-589. doi:10.1515/amm-2015-0177
67. Worldwide MI. A Basic Introduction to Rheology. *Whitepaper*. Published online 2016:1-19. <https://cdn.technologynetworks.com/TN/Resources/PDF/WP160620BasicIntroRheology.pdf>
68. Hersey MD. Future Problems of Theoretical Rheology. *J Rheol (N Y N Y)*. 1932;3(2):196-204. doi:10.1122/1.2116450
69. Eberhard U, Seybold HJ, Floriancic M, et al. Determination of the Effective Viscosity of Non-newtonian Fluids Flowing Through Porous Media. *Front Phys*. 2019;7. doi:10.3389/fphy.2019.00071

70. Sheng JJ. Polymer Flooding—Fundamentals and Field Cases. In: *Enhanced Oil Recovery Field Case Studies*. Elsevier; 2013:63-82. doi:10.1016/B978-0-12-386545-8.00003-8
71. Sisko AW. The Flow of Lubricating Greases. *Ind Eng Chem*. 1958;50(12):1789-1792. doi:10.1021/ie50588a042
72. Yasuda K. A multi-mode viscosity model and its applicability to non-Newtonian fluids. *J Text Eng*. 2006;52(4):171-173. doi:10.4188/jte.52.171
73. Janáková G. Biodegradable solid dispersion for application to mucous membranes. Published online 2019.
74. Andreopoulos AG, Hatzi E, Doxastakis M. Controlled release of salicylic acid from poly(D,L-Lactide). *J Mater Sci Mater Med*. 2001;12(3):233-239. doi:10.1023/a:1008911131657